Autonomous Navigation for Robot-Assisted Intraluminal and Endovascular Procedures: A Systematic Review

Ameya Pore , *Graduate Student Member, IEEE*, Zhen Li , *Graduate Student Member, IEEE*, Diego Dall'Alba , Albert Hernansanz, Elena De Momi , *Senior Member, IEEE*, Arianna Menciassi , *Fellow, IEEE*, Alicia Casals Gelpí , *Senior Member, IEEE*, Jenny Dankelman , *Member, IEEE*, Paolo Fiorini , *Life Fellow, IEEE*, and Emmanuel Vander Poorten , *Member, IEEE*

Abstract—Increased demand for less invasive procedures has accelerated the adoption of Intraluminal Procedures (IP) and Endovascular Interventions (EI) performed through body lumens and vessels. As navigation through lumens and vessels is quite complex, interest grows to establish autonomous navigation techniques for IP and EI for reaching the target area. Current research efforts are directed toward increasing the Level of Autonomy (LoA) during the navigation phase. One key ingredient for autonomous navigation is Motion Planning (MP) techniques. This paper provides an overview of MP techniques categorizing them based on LoA. Our analysis investigates advances for the different clinical scenarios. Through a systematic literature analysis using the PRISMA method, the study summarizes relevant works and investigates the clinical aim, LoA, adopted MP techniques, and validation types. We identify the limitations of the corresponding MP methods and provide directions to improve the robustness of the algorithms in dynamic intraluminal environments. MP for IP and EI can be classified into four subgroups: node, sampling, optimization, and learning-based techniques, with a notable rise in learning-based approaches in recent years. One of the review's contributions is the identification of the limiting factors in IP and EI robotic systems hindering higher levels of autonomous navigation. In the future, navigation is bound to become more autonomous, placing the clinician in a supervisory position to improve control precision and reduce workload.

Index Terms—Autonomy, continuum robots, endovascular interventions, intraluminal procedures, medical robotics, motion planning, navigation.

Ameya Pore is with the Department of Computer Science, University of Verona, 37134 Verona, Italy, and also with the Center of Research in Biomedical Engineering, Universitat Politècnica de Catalunya, 08034 Barcelona, Spain (e-mail: ameya.pore@univr.it).

Zhen Li is with the Department of Electronics, Information and Bioengineering, Politecnico di Milano, 20133 Milan, Italy, and also with the Department of Biomechanical Engineering, Delft University of Technology, 2628 Delft, The Netherlands (e-mail: zhen.li@polimi.it).

Diego Dall'Alba and Paolo Fiorini are with the Department of Computer Science, University of Verona, 37134 Verona, Italy (e-mail: diego.dallalba@gmail.com; paolo.fiorini@univr.it).

Albert Hernansanz and Alicia Casals Gelpí are with the Center of Research in Biomedical Engineering, Universitat Politècnica de Catalunya, 08034 Barcelona, Spain (e-mail: albert.hernansanz@upc.edu; alicia.casals@upc.edu).

Elena De Momi is with the Department of Electronics, Information and Bioengineering, Politecnico di Milano, 20133 Milan, Italy (e-mail: elena.demomi@polimi.it).

Arianna Menciassi is with The BioRobotics Institute, Scuola Superiore Sant'Anna, 56127 Pisa, Italy (e-mail: arianna@sssup.it).

Jenny Dankelman is with the Department of Biomechanical Engineering, Delft University of Technology, 2628 Delft, The Netherlands (e-mail: j.dankelman@tudelft.nl).

Emmanuel Vander Poorten is with the Department of Mechanical Engineering, KU Leuven, 3001 Leuven, Belgium (e-mail: Emmanuel.VanderPoorten@kuleuven.be).

Color versions of one or more figures in this article are available at https://doi.org/10.1109/TRO.2023.3269384.

Digital Object Identifier 10.1109/TRO.2023.3269384

I. INTRODUCTION

INTRALUMINAL procedures (IP) and endovascular interventions (EI) are emerging medical therapies that make use of body lumens and vessels to reach otherwise difficult-to-reach regions deep into the body (see Fig. 1). To enable these procedures, snake-like flexible instruments are needed that can adapt to the complex intraluminal and endovascular anatomy [1]. Intraluminal procedures and endovascular interventions (IPEI) have shown significant improvements in patient outcomes, such as reduced blood loss, postoperative trauma, wound site infection, and recovery/hospitalization time [2]. However, the flexible tools used in IPEI have nonergonomic designs. It is also difficult to control these instruments precisely as a complex mapping between input and output motion is present. This design limitation drastically increases the cognitive and physical workload of the clinician. Overall, it is well-known that clinicians undergo a long learning curve before becoming proficient in using such highly dexterous instruments [3].

IPEI are composed of several complex tasks that must be performed in the right order and following strict procedures. The first task (which may take a large proportion of time) consists of carefully navigating to reach the targeted area [4], [5]. A major challenge during this first navigation phase consists of the complexity of operating in a deformable but constrained workspace with a device that itself is quite compliant. The interventional instruments have to traverse the anatomical passageways. While doing so, they constantly keep contact with the lumen or vessels along at least a certain portion of their body length [2]. Such contacts generally happen outside the field of view due to
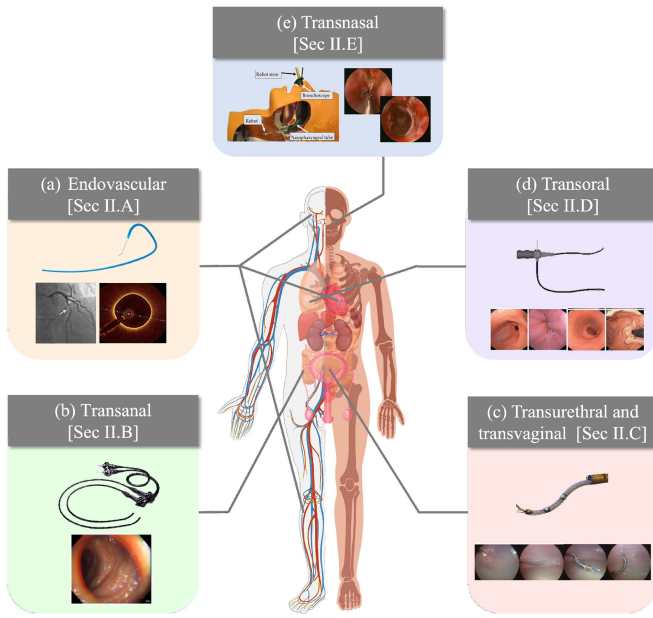
Fig. 1. IPEI considered in this article with respective standard interventional tools used and clinical target sites. (a) Endovascular catheterization. (b) Transanal colorectal procedures with a standard endoscope. (c) Transurethral and transvaginal access for prostate or bladder procedures. (d) Transoral procedures for airways or oesophagus. (e) Transnasal procedure to access bronchi. A primary difference between IP and EI is the sensing modalities used, i.e., IP commonly use images from a camera as sensory input, whereas EI mostly use X-Ray fluoroscopy.

restrictive perception of the endoluminal or endovascular tool architecture [6]. Contacts may be dangerous, and their response is generally hard to predict, especially when there is no direct sight of the local anatomy. Moreover, the movement of the tools is hard to predict. Movement at the proximal end may lead to no, limited or unexpectedly large movement of the distal tip [7]. Here, friction, slack, and deformation of the instrument and vascular or luminal wall prevent a desirable one-to-one relation between the proximal and distal tip motion.

All these aspects make navigation in IPEI very challenging, and robotic systems have been introduced to improve the current situation. However, the introduction of robotic assistance has only partially reduced the procedure complexity [8], due to nonintuitive mapping between user and robot motions, limits on tool dexterity and poor shape sensing capabilities affecting situational awareness [9]. It is believed that automation could provide benefits to reduce clinicians' workload while improving the overall outcome of the procedure [8], [9], [10]. For instance, navigation assistance could minimize path-related complications, such as perforation, embolization, and dissection, caused by excessive interaction forces between interventional tools and the lumen or vessels. Furthermore, with the increasing demand for IPEI and the limited number of experts [11], autonomous navigation will place clinicians in a supervisory role requiring minimal and discontinuous intervention. It will allow them to focus on high-level decisions rather than low-level execution.

An autonomy framework for robot-assisted minimally invasive surgical (MIS) was recently proposed with different levels of autonomy (LoAs) based on robot assistance, task automation, conditional autonomy, and high-level autonomy [12]. A detailed analysis of the framework mentioned previously was carried out by Haidegger et al. [10] and Attanasio et al.[9]

where they map out technologies that provide distinct features at different LoA for robot-assisted MIS. These studies use a top-down approach to define LoA based on general features of robot-assisted MIS. Hence, applying these levels for specific subtasks, such as navigation in IPEI is not trivial. A bottom-up granular approach is required to define LoA, considering specific clinical phases. Therefore, this article introduces a set of characteristic features essential for defining the LoA for the IPEI navigation phase. Characteristic features refer to subtasks associated with a specific clinical phase (i.e., IPEI navigation), such as target localization, motion planning, and motion execution. These characteristic features are used to define the LoA for the IPEI navigation. The inclusion of autonomous features raises several ethical and regulatory concerns due to incorrect robot behavior. This article discusses recent regulatory developments for high-risk applications, such as autonomous robotic systems in IPEI.

One of the initial steps toward enabling autonomous navigation for IPEI is through implementing motion planning (MP) techniques [13]. MP refers to obtaining a path from a start to a goal configuration, respecting a collision-free workspace.

It is a well-studied problem for rigid robotic manipulators [14]. Recent studies have explored MP for flexible continuum robots with a large number of degrees of freedom (DoFs) [15], [16]. However, there is a lack of an organized survey of MP for IPEI and other biomedical applications using continuum robotic systems. We consider the problem of a continuum robotic system operating in a clustered and highly variable environment relevant to IPEI scenarios. Thus, we conduct a survey of existing MP methods for IPEI, the associated challenges and potential promising directions. Capsule robots are excluded from this survey since they are generally used for imaging or drug delivery with limited diagnostic capabilities. We consider IPEI robots with diagnostic capabilities, a large proportion of which are continuum robots.

The contributions of this review article are, first, to identify the LoA for the IPEI navigation phase; second, to provide an overview of existing MP methods that could enable autonomous navigation; and third, to provide future directions toward autonomous navigation for IPEI. The rest of this article is organized as follows. Section II provides an overview of different IPEI considered in this work, the challenges associated and the robotic systems available. Section III describes the LoA for IPEI navigation and the recent regulatory measures developed. Section IV introduces the survey analysis for MP methods. It presents the taxonomy and classification of MP algorithms for IPEI procedures. Finally, the future development directions of IPEI navigation are proposed in Section V. Finally, Section VI concludes this article.

II. ROBOTIC AUTOMATION IN IPEI

IP can be categorized into endoluminal and transluminal procedures [6], [17]. Endoluminal procedures involve interventions whereby the instruments move through and stay in natural body orifices and lumens. In transluminal procedures, instruments operate in body lumens. However, they also can create incisions in lumen walls to access target sites beyond the lumen, such as natural orifice transluminal endoscopic surgery. Examples of endoluminal procedures include transoral interventions of the

airways or oesophagus, transanal access to the lower digestive tract, transnasal access to bronchi, and transurethral bladder and upper urinary tract procedures. Examples of transluminal procedures include transgastric and transvaginal abdominal procedures, transoesophagal thoracic, and transanal mesorectal procedures (see Fig. 1). In the context of this article, we use IP as an inclusive term for referring to both endoluminal and transluminal procedures. EI use a percutaneous approach to reach target areas in the vasculature. Typical EI include aneurysm repair, stent-graft, transcatheter aortic valve implantation, radio-frequency ablation, mitral valve repair, etc [18]. While the technical innovation for IPEI remains similar, EI are carried out typically using external image guidance, such as through X-Ray fluoroscopy or echography [17].

Some hospital units use consolidated robot-assisted MIS systems [19] for IPEI, however a large proportion of robotic systems consists of continuum robots [6], [16]. Continuum robots are actuated structures that form curves with continuous tangent vectors and are considered to have an infinite number of joints and DoFs [2], [16]. They have produced a step change in medical robotics as they offer better access and safer interactions making new interventions possible. However, they are highly complex to model, sense, and control [2]. Current robotic solutions for IPEI in the research phase are advancing the state-of-the-art through integrating new technologies that enhance the ability to recognize and interact with tissues through increased dexterity and sensory feedback [9]. These technological advances can help in navigation guidance and building higher LoA. Some systems are used in multiple procedures due to the lack of specific robotic technologies, multifunctionality and the ability of robotic systems to adapt to different IPEI procedures that share similar technical or clinical characteristics [20]. This section outlines the available robotic platforms for IPEI. Our study considers EI and transanal, transurethral, transvaginal, transoral, and transnasal procedures target clinical applications (see Fig. 2). We do not take into account procedures in which the development of continuum robotic systems is in its infancy or where the navigation phase does not constitute the predominant phase, such as auditory canal access, transvascular interventions, and exploratory procedures of the lymphatic system.

A. Endovascular Interventions

In a general EI, cardiologists introduce a guidewire through a small incision on the groin, the arm, or the neck. The guidewire is advanced to the desired location and acts as the stable track for the catheter to follow. Two major challenges in controlling catheters and guidewires exist in this procedure. One difficulty is steering guided through a 2-D fluoroscopy image [21], [22]. Hence, it requires a precise understanding of the 3-D anatomy projected in a 2-D image plane. The other difficulty is steering the instrument tip by combining insertion, retraction and torque actions at the proximal end of the catheter and guidewire. These actions give rise to haptic feedback due to friction and collision between the catheter and the vascular walls [23]. Robotic advancements in computer assistance, such as enhanced instrumentation, imaging, and navigation, have improved the current state of endovascular procedures. In addition, robotic platforms provide controlled steering of the catheter tip with improved stability. As a result, there is a growing interest in teleoperated
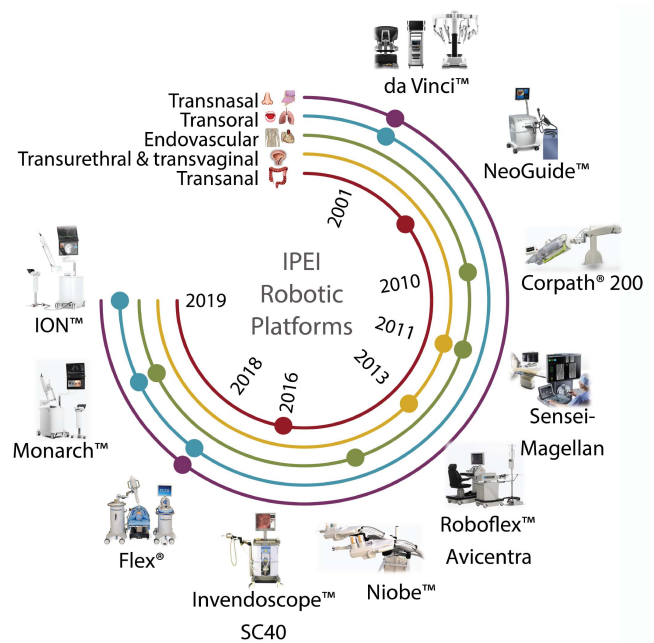

Fig. 2. Selection of some commercial robotic systems for Intraluminal Procedures and Endovascular Interventions (IPEI). For EI: Corpath system (Corindus, Waltham, USA) and Niobe system (Stereotaxis, St. Louis, USA), Sensei–Magellan (Hansen Medical, Mountain View, USA) and Monarch system (Auris Health, Redwood, USA); For transurethral and transvaginal procedures: Roboflex (ELMED, Ankara, Turkey) and Sensei–Magellan (Hansen Medical, Mountain View, USA); For gastrointestinal transanal procedures: Invendoscope (Invendo Medical, Weinheim, Germany) and Aer-O-Scope (GI View Ltd, Ramat Gan, Israel); For transnasal procedures: da Vinci (Intuitive Surgical, Sunnyvale, USA) and Flex (Medrobotics, Raynham, USA) For bronchoscopic transoral intervention: Monarch system (Auris Health, Redwood, USA), ION (Intuitive Surgical, Sunnyvale, USA), da Vinci (Intuitive Surgical, Sunnyvale, USA), and Flex (Medrobotics, Raynham, USA) are used.

robotic catheterization systems, which offer reduced radiation exposure, increased precision, elimination of tremors, and added operator comfort.

Recent developments in CorPath GRX (Corindus, Waltham, USA) provide guided robotic control that allows clinicians to navigate endovascular tools through a joystick. Other robotic catheter systems formerly introduced by Hansen Medical (Mountain View, USA) and later acquired by J&J robotics (New Brunswick, USA) are the Sensei X and Magellan platforms. Although used for different cardiovascular applications, they are not commercially available anymore. These platforms are considered in the article since they were milestones in robotic systems for EI [20]. Part of this technology entered into the Monarch platform (Auris Health, Redwood, USA), which targets bronchoscopy. The mechanically driven Amigo (Catheter Robotics Inc. Budd Lake, USA) and the R-One (Robocath, Rouen, France) robotic assistance platform allows steering standard catheters in three DoFs using an intuitive remote controller that replicates the standard handle of a catheter. The Niobe (Stereotaxis, St. Louis, USA) is a remote magnetic navigation system in which a magnetic field guides the catheter tip. The tip deflection is controlled by changing the orientation of outer magnets by utilizing a mouse or a joystick at the workstation. These robotic systems have reported excellent intravascular navigation. However, the absence of haptic feedback affects the procedural outcome when manoeuvring in smaller vessels, such as coronary, cerebral, and visceral vessels [24], [25].

B. Transanal IP

Transanal colonoscopy is a widely used method for the diagnosis and treatment (screening and surveying) of colonic diseases, such as colorectal cancer (CRC) [7], [26]. In a standard colonoscopy procedure, an insertion tube is introduced through the anus and pushed forward to inspect the colonic wall [27]. Early detection and diagnosis of CRC lesions is essential for improving the overall outcome of the patient [7], [27]. The rise in the number of colonoscopies has increased the workload of endoscopists. However, not enough attention is given to the ergonomic aspects of conventional colonoscopy. Several studies have reported work-related musculoskeletal injuries of the hand, wrist, forearm, and shoulder among colonoscopists [28], [29]. Although colonoscopy-related adverse events rarely occur, the proportion of subjects with risk factors is increasing. Severe colonoscopic complications, such as perforation and bleeding, can be fatal [30], [31]. Furthermore, even well-experienced endoscopists are often limited by the lack of manoeuvrability, which can result in about 20% of missed polyp localization [32]. The rate of missed polyp detection varies by the polyp type, often early-stage malignancies being difficult to detect [33].

Robotic colonoscopy has been investigated to simplify the use of flexible endoscopes, reducing the procedure time and improving the overall outcome of the procedure [26]. Some cost-efficient solutions have shown advantages in reducing pain, the need for sedation, and the possibility of being disposable [7]. These platforms have a self-propelling semiautonomous or teleoperated navigation system. Several robotic colonoscopy platforms have received clearance to enter the market. These include the NeoGuide Endoscopy System (NeoGuide Endoscopy System Inc., Los Gatos, USA) [34], the Invendoscope E210 (Invendo Medical GmbH, Weinheim, Germany), the Aer-O-Scope System (GI View Ltd., Ramat Gan, Israel) [35], the ColonoSight (Stryker GI Ltd., Haifa, Israel) [36], and the Endotics System (ERA Endoscopy Srl, Pisa, Italy) [37]. The NeoGuide Endoscopy system and the ColonoSight are no longer commercially available. The Neoguide system is a cable-driven system that consists of 16 independent segments with two DoFs each, position sensors at the tip to obtain the insertion depth and real-time 3-D mapping of the colon. Whereas the Invendoscope E210 is a single-use, pressure-driven colonoscope that grows from the tip using a double layer of an inverted sleeve, reducing the forces applied to the colonic wall. The device has a working channel with electrohydraulic actuation at the tip. The ColonoSight is composed of a reusable endoscope wrapped with a disposable sheath to prevent infection. The locomotion is provided by the air inflated inside the sleeve that covers an inner tube. The tip consists of a bendable section with two working channels. The Aer-O-Scope is a disposable self-steering and propelling endoscope that uses electropneumatic actuation through two sealed balloons. Recent proof-of-concept of the device showed successful caecum intubation with no need for sedation [35]. The endotic system uses a remotely controlled disposable colonoscope that mimics inchworm locomotion.

C. Transurethral and Transvaginal IP

Transurethral interventions have been used generally for bladder cancer resection, radical prostatectomy, and partial cystectomy [38]. Transvaginal access has been utilised for nephrectomy [39]. Both these interventions use an endoscopic device to intentionally puncture a viscera (e.g., vagina, ureter, and urinary bladder) to access the abdominal cavity and perform intra-abdominal operations [40]. There are considerable challenges that limit the widespread adoption of transurethral and transvaginal access for urological applications, such as the unmet need for dedicated specially designed instruments resulting in lack of distal dexterity, limited tool accuracy, and limited depth perception [39], [41]. These factors lead to the underresection of tumours and difficulty in enucleating tissue with minimal tilting of the rigid tools and the urethral anatomy, motivating research in robot-assisted techniques [38].

In 2008, robotic flexible ureteroscopy (fURS) was accomplished using the Sensei–Magellan system (Hansen Medical, Mountain View, USA), which was designed for cardiology and angiography [42]. Since 2010, ELMED (Ankara, Turkey) developed the Roboflex Avicenna for fURS that directly drives the endoscope and an arm enabling rotation by a joystick. Compared to traditional flexible ureteroscopy, this system's advantage lies in improved movement precision and better ergonomics [43].

D. Transoral IP

Conventional transoral endoscopy (TOE) is the standard diagnostic method used to examine the oesophagus, stomach, and proximal duodenum. In TOE, varying lengths of flexible endoscopes are used, e.g., gastroscopes (925 mm–1.1 m), Duodenoscopes (approximately 1.25 m), and Enteroscopes (1.52–2.2 m) [44]. The diagnostic and therapeutic capabilities of TOE strongly correlate with the technical and decision-making skills of the operator with a steep learning curve [45]. Standard endoscopic surgical approach for laryngeal lesions uses laryngoscope, microscope, and laser [46]. This approach requires the surgeon to work within the limits of the laryngoscope and gain line-of-sight observation to complete the operation [46]. Transoral access is also used for bronchoscopy to reach the lungs farther down the airways. Conventionally, a bronchoscope is used for such procedures [47]. However, the average diagnostic yield remains low because of limited local view in the peripheral airways [48]. Electromagnetic navigation was introduced to guide the bronchoscope through the peripheral pulmonary lesions, but it lacked direct visualization of the airways, hence motivating the need for robotic assistance [49].

Available robotic systems for TOE includes the EASE system (EndoMaster Pte, Singapore) and EndoSamurai (Olympus Medical Systems Corp., Tokyo, Japan). The EASE system is based on a teleoperated device that remotely controls the endoscopic medical arms. The EndoSamurai system consists of instruments mounted at the end of the endoscope for submucosal dissection procedures. Some other robotic systems in an early development phase are reviewed in [45].

Commercially available systems for laryngeal procedures are the da Vinci Robotic System (Intuitive Surgical, Sunnyvale, USA) and the Flex Robotic System (Medrobotics, Raynham, USA) [19]. The Flex robotic system includes a rigid endoscope controlled through a computer interface, with two external channels for flexible instruments.

In robotic bronchoscopy, Monarch (Auris Health Inc, Redwood, USA) is pioneering robotic endoscopy. The platform consists of an outer sheath, an inner bronchoscope with four DoF

steering control, electromagnetic navigation guidance and continuous peripheral visualization [49]. Another robotic platform called ION endoluminal system by intuitive surgical includes an articulated, flexible catheter with shape sensing capabilities, which provides positional and shape feedback along with a video probe for live visualization while driving the catheter. [49].

E. Transnasal IP

Systems for the transnasal procedure have been investigated with several exploratories in mind. These procedures, ranked according to the distance to the target from the entry point include transnasal navigation for sinuses, transnasal skull base procedure, and transnasal microprocedure of the upper airways.

One of the challenges with diseases of the sinuses lies in the difficulty of monitoring their progression, obtaining a biopsy, and facilitating intervention in the frontal and maxillary sinuses while avoiding visible scarring or obliteration of bone scaffolds of the nose. Conventionally, a flexible endoscope is used in clinical practice [50]. Skull-base surgeries are carried out through transnasal access. A typical target for these surgeries is the removal of pituitary gland tumours through a transsphenoidal approach [51], [52]. The standard endoscopic approach for these surgeries is limited by restricted access, cumbersome manual manipulation of interventional tools near susceptible anatomy and lack of distal dexterity [53].

Another interventional target using transnasal access is the upper airways and throat [54]. Transnasal endoscopy (TNE) is performed using an ultrathin endoscope with a shaft diameter of 6 mm. which is inserted through the nasal passage. Once the instrument is beyond the upper oesophageal sphincter, endoscopy is conducted in the standard fashion. However, there are some technical limitations of TNE, namely, a smaller working channel can result in limited suction and the availability of fewer endoscopic accessories.

In general practice, the robotic systems mentioned in transoral approaches, such as da Vinci Robotic System (Intuitive Surgical, Sunnyvale, USA) and Flex Robotic System (Medrobotics Corp., Raynham, USA) are also used in transnasal interventions [19]. The Flex Robotic System is an operator-controlled flexible endoscope system primarily designed for an ear–nose–throat procedure that includes a steerable endoscope and computer-assisted controllers, with two external channels for the use of compatible 3.5 mm flexible instruments. However, specific robotic systems with appropriate ergonomics and dimensions suited for transnasal passage are still under development [19].

III. LEVELS OF AUTONOMY

One of the promising features of upcoming IPEI robotic systems is autonomy since it provides the ability to perceive, analyze, plan, and take actions automatically [55]. An autonomous robotic system can deal with nonprogrammed situations and has the capability of self-management and self-guidance [56]. The most notable aspect of autonomy is the transfer of decision-making from a human operator to a robotic system. To allow this transfer, two conditions must be met [57]. First, the operator must transfer the control to the robotic system, including the related responsibilities (i.e., the human operator must "trust" the autonomous system). Second, the system must be certified, i.e., it must fulfill all ethical, legal, and certification requirements.

However, these certification standards are not fully developed for medical robotic systems due to a lack of consideration, and clear understanding of autonomy [58]. Therefore, we first introduce the ethical and regulatory aspects related to autonomy in Section III-A, then we define generic LoA in Section III-B, while in Section III-C, we present the specific LoA for IPEI navigation systems.

A. Ethical and Regulatory Aspects of Autonomy

The ethical concerns can be addressed from multiple perspectives, including human rights, law, economics, policy, and ethics [59]. We highlight the viewpoints of medical robot practitioners. When transferring the decisions from a human operator to an autonomous system, one of the main ethical concerns is the consequences of errors resulting from the decisions taken. These errors can be due to incorrect robot behaviors, leading to hazardous situations [60]. Hence, robot-assisted intervention is considered a high-risk category [61]. To address the ethical concerns, the European Commission proposed a regulatory framework for AI applications in the high-risk category, known as the Artificial Intelligence Act (AI Act) [61]. Similar efforts are being formalized in the United States under the National AI Initiative [62]. The AI Act describes the role of a human operator: the obligation to provide human supervision, the right for a human to override an automated decision, and the right to obtain human intervention, which forbids full autonomy. Therefore, human intervention needs to be carefully designed into the system at different levels of integration [63]. Furthermore, the reliability of medical robotics is associated with the notion of certification, which requires legal approval that the system has reached a particular standard. Several regulatory standards exist in the robotics domain; for instance, the standards for medical electrical systems are defined by the International Electrotechnical Commission (IEC) in the technical report (TR) 60601-4-1 [64], which guides risk management, basic safety, and essential performance toward systems with some degrees of autonomy. These regulatory standards are not fully developed for robot-assisted intervention, and the introduction of LoA could support this development by facilitating the system verification and validation with improved risk management [58]. As a consequence of upcoming regulations, such as the AI Act, it is expected that earlier phases of the design process will progressively consider safety and system integration concerns.

B. LoA: Definition

Quantifying system autonomy based on its capabilities presents a significant challenge due to different levels of advances in underlying technologies. In medical robotics, as the autonomous capabilities of the robot are increasing, the role of medical specialist is shifting from manual dexterity and interventional skills toward diagnosing and high-level decision-making.

Prior work identified five LoA for medical robot systems considering a complete clinical procedure and the capability of a human operator/clinician [10], [12]. At level 0, the robot has no decision autonomy, and the clinician controls all aspects of the system, i.e., the clinician exclusively controls it. At level 1, the robot can assist the clinician, while at level 2, it can autonomously perform an interventional subtask. At level 3, the robot can autonomously perform longer segments of the clinical

procedure while making low-level cognitive decisions. Finally, at level 4, the robotic system executes the complete procedure based on human-approved clinical plans or surgical workflow. Few studies have defined level 5, which refers to full autonomy in which the robotic clinician can perform the entire procedure better than the human operator; hence human approval is not required [10], [12]. However, level 5 is still in the realm of science fiction, so we consider it outside the scope of this article. In higher LoA, the robot responding to various sensory data will be highly sophisticated while it could replicate the sensorimotor skills of an expert clinician more closely.

Attanasio et al. [9] outlined the enabling technologies and the practical applications for different levels. Haidegger et al. [10] provided a top-down classification of LoA for general robot-assisted MIS. Their classification considers four robot cognitive functions (i.e., generate, execute, select, and monitor options), where the overall LoA is the normed sum of the four system functions assessed on a linear scale, "0" meaning fully manual and "1" fully autonomous.

In clinical practice, an interventional procedure workflow is decomposed into several granular levels, such as phase, steps, and gestures [65]. Many of the interventional phases and skills that are used in robot-assisted MIS are not considered in IPEI, e.g., luminal navigation. Hence, LoA defined for robot-assisted MIS cannot be directly applied for IPEI. Moreover, using the proposition provided by Haidegger et al., it is challenging to identify a clear boundary between human and automated control required for specific phases/steps of robot-assisted MIS. It introduces an additional problem of defining the system's overall level that implements different LoA for different phases of the procedure. Hence, we propose a bottom-up solution where an intermediate LoA is defined for specific interventional phases. Having knowledge of a subtask will enable a better understanding of the amount of human intervention required at a granular scale. A bottom-up classification would better estimate the overall system autonomy since underlying phases can be at a different intermediate LoA. Moreover, it can be applied to all medical procedures, from robot-assisted MIS to IPEI. The target of this article is IPEI navigation; hence we define the intermediate LoA for this interventional phase.

C. LoA for IPEI

LoA for robot-assisted MIS has been derived from the degree of autonomy introduced by ISO, who, jointly with IEC, created a TR (IEC/TR 60601-4-1) [64] to propose an initial standardization of autonomy levels in medical robotics. The report parameterizes DoFs along a system's four cognition-related functions: generate, execute, monitor, and select options strategy. A similar classification approach has been followed by Haidegger et al. for robot-assisted MIS. We identify the following three specific cognitive functions for an IPEI navigation task. 1) Target localization. 2) Motion planning. 3) Execution and replanning. Target localization is usually based on preoperative images, such as computed tomography (CT), magnetic resonance imaging (MRI), or X-Ray imaging. It is a critical feature, as inaccurate target identification can lead to inaccuracies in the subsequent steps. MP can be considered in two phases: preoperative and intraoperative. Preoperative MP refers to the planning performed before the procedure based on multimodal medical images [66].

This may be done in static virtual models of the lumen or vessels. Execution and replanning is an intraoperative phase to carry out the required motion to reach the target while continuously replanning intraoperatively. It can include target relocalization when adjustment is needed due to unexpected situations.

Table I illustrates the LoAs defined for IPEI navigation. In LoA 0, all the features from target localization, MP and motion execution are carried out by a human operator. Commercially available robotic system (as described in Section II) can be considered in this category since the human operator has complete control of the robotic motion. LoA 1 is characterized by target localization and preoperative planning manually carried out by the clinician. The clinician executes the actual motion with the assistance of the robotic system. Systems that use external tracking devices and registration methods to align the preoperative data with the intraoperative condition and support the clinician in executing a clinical procedure can be considered LoA 1 [67], [68], [69]. Taddese et al. [70] developed a tele-operated magnetically controlled endoscope, where the system provides navigation assistance by controlling the magnetic field. These systems represent the first implementations of LoA 1, where the manipulator executes the command imparted by the operator. In LoA 2, the robotic system fully controls the specific navigation steps. Target localization is carried out by the clinician, who provides input in the form of waypoints or demonstration trajectories. The path planner uses these cues to generate a global trajectory. Further, the robotic system carries out the required motion indicated by the path planner. During execution, the human operator supervises the autonomous navigation and approves the robot's actions or overrides it (to comply with AI Act indications). In LoA 3, after target localization by the clinician, the path planner generates the global path in the preoperative phase without any manual intervention. This level includes automatically splitting the entire navigation task into specific subtasks that could be performed autonomously. The robotic system executes the motion indicated by the path planner and adapts to environmental changes through real-time replanning. The local real-time knowledge will provide information regarding the anatomical environment, and the motion will be adjusted as the autonomously steering is performed. All the features from target localization, MP, and execution are autonomously carried out without any human intervention by a system reaching LoA 4. The main difference between LoA 3 and LoA 4 is the addition of automatic target identification. This additional feature requires enabling technologies, such as autonomous segmentation of organs to detect abnormal tissues, such as polyps, automatic localization, and shape sensing mechanisms [8] (see Section V-B). Fig. 3 shows a case study of LoA for the transanal IP. In the next section, the proposed LoA will be used to classify all the work considered in the field of IPEI navigation.

IV. SYSTEMATIC REVIEW OF MP FOR IPEI

A. Literature Review

A systematic analysis was conducted, following the PRISMA methodology [71], to survey the developments of automation and MP in IPEI.

TABLE I
DESCRIPTIVE CLASSIFICATION OF LoA FOR IPEI NAVIGATION. H: PERFORMED BY A HUMAN OPERATOR, M: PERFORMED BY A MACHINE. H/M: PERFORMED BY A HUMAN, ASSISTED BY A MACHINE, M/H: PERFORMED BY A MACHINE, ASSISTED BY A HUMAN. M^1: PERFORMED UNDER HUMAN SUPERVISION

| LoA	Description	Target localisation	Motion planning	Execution & re-planning
0	*Direct robot control*: The clinician exclusively controls all cognitive functions without any support or assistance [12]. Most IPEI systems used in clinical practice operate at Level-0 autonomy.	H	H	H
1	*Navigation assistant*: The human operator maintains continuous control of the robotic navigation intraoperatively; however, it is assisted robotically during the execution of the motion. Other cognitive functions are carried out manually.	H	H or M	H/M
2	*Navigation using waypoints*: The operator provides discrete high-level navigation tasks, such as waypoints or predefined trajectories. These trajectories are derived during preoperative planning. The robot carries out the required motion between the waypoints during the execution time, with the clinician in a supervisory role to approve or override the strategy.	H	M/H	M^1 or M/H
3	*Semi-autonomous navigation*: The final goal of navigation is provided by a human operator, and the system generates the strategies required to carry out the complete navigation task. During the execution time, it relies on the operator's supervision to approve or override the choice. In IPEI navigation, the robot would extract waypoints and then plan the trajectory to reach the point.	H	M	M^1
4	*High-level autonomous navigation*: This level is characterized by the ability of the system to make clinical decisions and execute the control solution under the clinician's supervision. The system should interpret preoperative imaging modalities such as CT, MRI and ultrasound to detect target regions and extract all the information required for proper navigation.	M	M	M^1
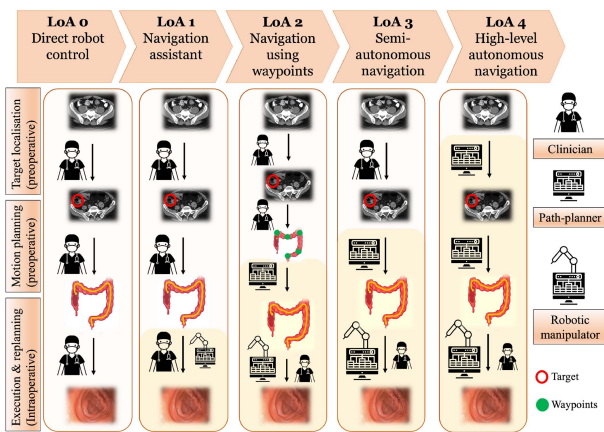
Fig. 3. Case study of LoA for endoscopic navigation for transanal IP. The complete navigation task is divided into three cognitive functions: target localization through preoperative imaging, planning the motion preoperatively and executing the motion. (Row 1) Target localization using preoperative images: The identified target is depicted with a red circle. (Row 2) Preoperative MP: Path representation inside the colon shown with a yellow line. (Row 3) Intraoperative motion execution and MP: Intraoperative endoscopic visualization. (left to right). LoA0-LoA4, respectively. For each level, we indicate the agent that operates each cognitive function. Agent refers to either a human operator, path-planning system, or robotic manipulator. In the case of two agents, the supervisor agent is depicted on the right-hand side, while the main agent executing the actions is on the left and its icon is larger.

Fig. 4. (a) Search matrix used for the survey. (b) Prisma flow diagram summarizing how the systematic review was conducted.

1) Search Method: A systematic analysis was conducted using the following digital libraries. `Google Scholar`, `Scopus`, and `IEEE Xplore`. Search queries were programmatically generated from the search term matrix. Query results were automatically retrieved and checked for duplicates via the `Scopus` API. The list of references was saved as a . *csv* file and manually evaluated according to the inclusion criteria. All items that did not meet the inclusion criteria were excluded. The search terms used in this survey were chosen by generalizing the term "motion planning for intervention."
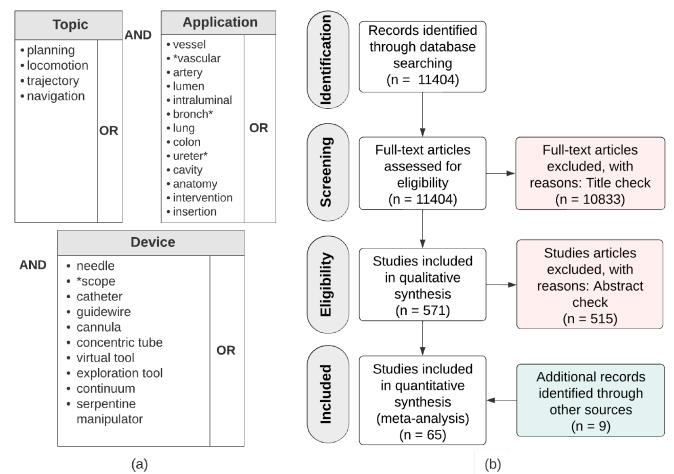
Search terms are combined with the logical operators AND and OR such that a large search space can be covered in sufficient detail. Fig. 4 provides an overview of all the search terms and the flow of the conducted review. This matrix, once all possible combinations have been exhausted, yields 520 entries. To automatically manage all the generated entries and remove the duplicates, a python library, pybliometrics, was used [72]. The cutoff date for the earliest work included is 2005, and the latest work is from July 2022.

2) Selection Criteria: This article was selected by:
  i) considering only continuum robots (excluding capsule mobile robots [73], [74]) for IPEI;
  ii) excluding low-level controller studies based on force control, position control, impedance control, and similar;
  iii) considering only full papers drafted in English. Extended abstracts reporting preliminary findings were omitted;
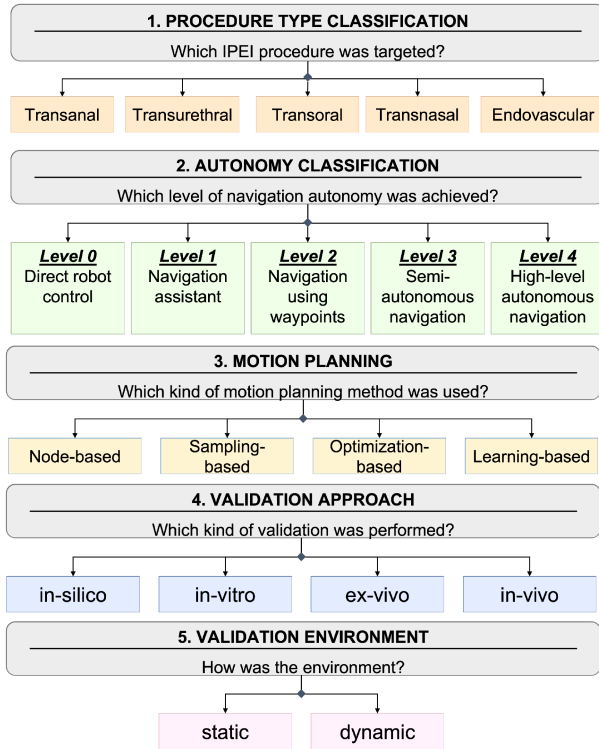
Fig. 5. Schematics of the analysis carried out for each paper. These criteria include the targeted procedure, the LoA, the MP method, the validation, and the dynamics of the environment.
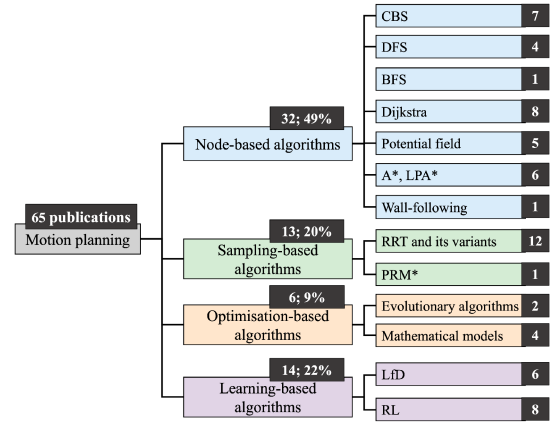

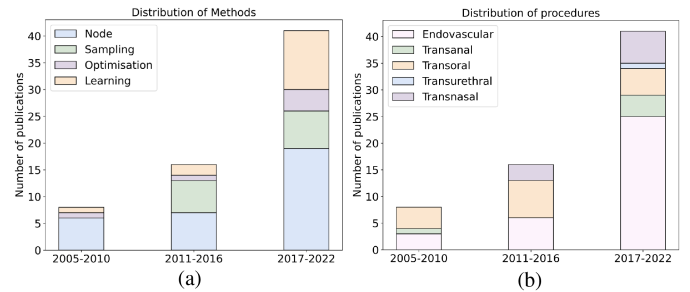Fig. 6. Classification of IPEI MP methods for continuum robots found in literature.

Fig. 7. Chronological development of endoluminal navigation. (a) MP approaches. (b) Targeted IPEI procedures. Until 2010, the majority of studies have implemented node-based and sampling algorithms for MP. While lately, with the exponential increase in computational resources, the field is transitioning toward learning-based methods.

iv) excluding transluminal procedures that require incisions, such as hydrocephalus ventricles.

3) Postprocessing and Analysis: The search script returned 11 404 references. Prisma flow diagram in Fig. 4(b) summarizes how the systematic review was conducted. 10 833 references and 515 references were excluded after title check and abstract check, respectively. Additional nine references were included manually because search results did not cover 100% of the current studies for different reasons. Finally, this process yielded a list of 65 references.

The outcomes of various studies were classified based on several criteria, shown in Fig. 5, including the targeted procedure, the LoA, the MP method, the validation, and the environment's dynamics. The MP methods are categorized into subgroups presented in Fig. 6 for an in-depth analysis. The summary of the state-of-the-art on IPEI MP publications are presented in Table III, and its development is shown in Fig. 7(a). Besides the MP approach, we have highlighted the distribution of the targeted IPEI procedures in Fig. 7(b). Moreover, Table III shows that some studies involved intraoperative path replanning with a dynamic environment (last column).

B. Taxonomy on MP for IPEI Navigation

MP has been a well-documented field for navigation tasks since the 1980s, supporting robotic manipulators and mobile platform operations in indoor and outdoor industrial applications. During MP, robot characteristics are usually considered

to find a feasible path solution, such as its geometrical dimensions to avoid collisions and kinematic constraints to respect its movement capability. The robot kinematics describes the relationship between the configuration and task spaces [75]. The configuration space $\mathscr{C}$ is defined as all robot configurations. The task space $\mathscr{T}$ is referred to as the workspace that the robot can reach for each specific configuration $\mathbf{q}$. The robot kinematics can be expressed in a general form as

$$\mathscr{T} = f(\mathbf{q}) \quad \mathbf{q} \in \mathscr{C}. \tag{1}$$

MP is an essential component of autonomous IPEI robotic systems, even under complex operating conditions and stringent safety constraints. As shown in Fig. 6, MP methods can be decomposed into four subgroups by adjusting the taxonomy of path planning in general robots from [76]: node, sampling, optimization, and learning-based techniques. The node-based (or graph-based) algorithms use a graph-searching strategy along with a tree structure. The sampling-based algorithms construct a tree structure based on random samples in a configuration space. Therefore, these methods find a collision-free path and ensure compatibility with the robot's motion capabilities. Optimization-based algorithms formulate the MP problem as a mathematical problem by minimizing or maximizing an objective function with respect to some constraints and obtaining the optimal case through a solver. Learning-based methods use a Markov decision process to learn a goal-directed policy based

TABLE II
BACKGROUND OF PATH-PLANNING METHODS

No.	Path Planning	Description
1.	**Node-based**	
a.	Centerline-based structure (CBS)	CBS algorithm approximates the path closest to the centerline, i.e., the path that maximizes the distance from all obstacles in the environment. This method builds a tree model of the environment, where each node contains its circular/spherical approximation (i.e. position of the center and local radius from the wall).
b.	Depth first search (DFS)	DFS algorithm traverses a graph by exploring as far as possible along each branch before backtracking [77]
c.	Breadth first search (BFS)	BFS algorithm [78] starts at the tree root and explores the k-nearest neighbour nodes at the present depth before moving on to the nodes at the next depth level.
d.	Dijkstra	The Dijkstra algorithm [79] is an algorithm for finding the shortest paths between nodes in a graph. It is also called Shortest Path First (SPF) algorithm. The Dijkstra algorithm explores a graph by expanding the node with minimal cost.
e.	Potential field	Artificial potential field algorithms [80] define a potential field in free space and treat the robot as a particle that reacts to forces due to these fields. The potential function is composed of an attractive and repulsive force, representing the different influences from the target and obstacles, respectively.
f.	A* and lifelong an-ning A* (LPA*)	A-star [81] is an extension of the Dijkstra algorithm, which reduces the total number of states by introducing heuristic information that estimates the cost from the current state to the goal state.
g.	Wall-following	Wall-following algorithms move parallel and keep a certain distance from the wall according to the feedback received from sensors.
2.	**Sampling-based**	
a.	Rapidly-exploring random tree (RRT)	RRT [82] and its derivatives are widely used sampling-based methods. These methods randomly sample in the configuration space or workspace to generate new tree vertices and connect the collision-free vertices as tree edges. In addition, these methods can consider the kinematic constraints (i.e., curvature limitations) during MP.
b.	Probabilistic roadmap* (PRM*)	A probabilistic roadmap is a network graph of possible paths in a given map based on free and occupied spaces [83], [84]. PRM* takes random samples from the robot's configuration space, tests them for whether they are in the free space, and uses a local planner to attempt to connect these configurations to other nearby configurations. Then, the starting and goal configurations are added in, and a graph search algorithm is applied to the resulting graph to determine a path between these two configurations.
3.	**Optimization-based**	
a.	Mathematical model	MP can be formulated as a path optimization problem with constraints on the robot model, such as its kinematic model [85]. The mathematical model optimizes an objective function that exists within equality and inequality constraints and is solved by linear or nonlinear programming.
b.	Evolutionary algorithms	Evolutionary algorithms use bio-inspiration to find approximate solutions to difficult optimization problems. Ant Colony Optimization (ACO) is one of the population-based metaheuristic algorithms [86]. Artificial ants incrementally build solutions biased by a pheromone model, i.e. a set of parameters associated with graph components (either nodes or edges) whose values are modified at runtime by the ants. Genetic Algorithm (GA) is another bio-inspired evolutionary algorithm [87], where the initial population comprises multiple chromosomes, and each chromosome is composed of several genes representing optimization variables. The population is updated by crossover and mutation of genes. Finally, the optimal solution is selected from the population after several generations.
4.	**Learning-based**	
a.	Learning from Demon-strations (LfD)	LfD is the paradigm where an agent acquires new skills by learning to imitate an expert. LfD approach is compelling when ideal behaviour cannot be easily scripted, nor defined easily as an optimisation problem, but can be demonstrated [88].
b.	Reinforcement learn-ing (RL)	In RL, an agent learns to maximise a specific reward signal through trial and error interaction with the environment by taking actions and observing the reward [89].

on a reward function. A brief general definition of different MP methods is provided in Table II, while Table III summarizes different MP works for IPEI applications.

1) Node-Based Algorithms: Node-based algorithms use an information structure to represent the environment map and are commonly used for navigation assistance [76]. Table III shows different MP works for IPEI that exploit node-based methods. As schematized in Fig. 6, algorithms that have been adopted here are centerline-based structure (CBS), depth first search (DFS), breadth first search (BFS), Dijkstra, potential field, A*, lifelong planning A* (LPA*), and wall-following.

a) Centerline-based structure: Geiger et al. [90] extracted the 3-D skeleton for bronchoscopy planning by computing the skeleton of the segmented structure and then converting this skeleton into a hierarchical tree model of connected branches. Sánchez et al. [91] obtained the skeleton of the bronchial anatomy via the fast marching method first and then defines the skeleton branching points as a binary tree (B-tree). Sánchez' study gives a path corresponding to a sequence of nodes travers-ing the B-tree. Intraoperatively, a geometry likelihood map is used to match the current exploration to the path planned preop-eratively. The airway centerlines serve as the natural pathways for navigating through the airway tree. They are represented by a discrete set of airway branches in [67]. Starting with each target region of interest (ROI) associated airway route, the method from Khare et al. [67] automatically derives a navigation plan that consists of natural bronchoscope manoeuvres abiding by the rotate-bend-advance paradigm learned by physicians during their training. This work is evaluated both in phantoms and in a human study.

Wang et al. [92] developed a method to build a navigation in-formation tree based on the vasculature's centerline for catheter-ization. The authors made a tree structure assuming the vascular system was rigid and interrogated the tree to find the nearest node during intraoperative navigation. The navigation experiments were carried out on a resin vessel phantom. Another study proposed a 3-D vasculature's centerline extraction approach via a Voronoi diagram [93]. It treated the centerlines as the minimal action paths on the Voronoi diagrams inside the vascular model surface. The experimental results show that the approach can extract the centerlines of the vessel model. Further Zheng et al. [68] first proposed to extract the preoperative 3-D skeleton via a parallel thinning algorithm for medical axis extraction [94]. Second, they proposed to use a graph matching method to establish the correspondence between the 3-D preoperative and 2-D intraoperative skeletons, extracted from 2-D intraoperative fluoroscopic images. However, the proposed graph matching is sensitive to topology variance and transformation in the sagittal and transverse planes. A recent study on transnasal exploration proposed central path extraction algorithm based on preplanning for the roaming area [95].

Nevertheless, a common disadvantage of work available in the literature describing this approach is that they focus on constructing an information structure, but path exploration in-side the information structure is not mentioned [67], [68], [90], [91], [92], [93]. Specifically, the tree structure is built, but the

TABLE III
SUMMARY OF MOTION PLANNING METHODS FOR IPEI NAVIGATION

Ref.	Procedure	Method	Robot	Kinematics	Validation	Environment
Level 1: Navigation assistant						
Node-based:						
[90] Geiger 2005	Transoral	CBS	Bronchoscope	N	in-silico (3-D pulmonary vessels)	Static
[100] Schafer 2007	Endovascular	Dijkstra	Guidewire	N	in-vitro (3-D cardiovascular)	Static
[101] Egger 2007	Endovascular	Dijkstra	Catheter	N	in-silico (3-D aorta)	Static
[103] Gibbs 2007	Transoral	Dijkstra	Bronchoscope	N	in-silico (3-D bronchus)	Static
[104] Gibbs 2008	Transoral	Dijkstra	Bronchoscope	N	in-silico (3-D bronchus)	Static
[102] Liu 2010	Endovascular	Dijkstra	Catheter	N	in-vitro (3-D aorta)	Static
[92] Wang 2011	Endovascular	CBS	Catheter	N	in-vitro (3-D resin vessel)	Static
[98] Huang 2011	Endovascular	DFS	Guidewire	N	in-silico (3-D aorta)	Static
[108] Rosell 2012	Transoral	Potential field	Bronchoscope	Y	in-silico (3-D tracheobronchial)	Static
[97] Gibbs 2013	Transoral	DFS	Bronchoscope	Y	in-vivo (3-D bronchus)	Dynamic
[93] Yang 2014	Endovascular	CBS	Guidewire	N	in-silico (3-D aorta)	Static
[67] Khare 2015	Transoral	CBS	Bronchoscope	Y	in-vivo (3-D bronchus)	Dynamic
[91] Sánchez 2016	Transoral	CBS	Bronchoscope	N	in-silico (3-D bronchus)	Static
[68] Zheng 2018	Endovascular	CBS	Catheter	N	in-vitro (3-D aorta)	Dynamic
[114] Ciobirca 2018	Transoral	A*	Bronchoscope	N	in-silico (3-D bronchus)	Static
[115] Niyaz 2018	Transnasal	LPA*	Concentric tube robot	Y	in-silico (3-D nasal cavity)	Static
[116] Niyaz 2019	Transnasal	LPA*	Concentric tube robot	Y	in-silico (3-D nasal cavity)	Static
[69] Zang 2019	Transoral	DFS	Bronchoscope	Y	in-vivo (3-D bronchus)	Dynamic
[109] Yang 2019	Transurethral	Potential field	Ureteroscope	Y	in-silico (3-D ureter)	Static
[120] Fagogenis 2019	Endovascular	wall-following	Concentric tube robot	Y	in-vivo (3-D cardiovascular)	Dynamic
[113] He 2020	Transnasal	A*	Endoscope	N	in-silico (3-D nasal cavity)	Static
[96] Zang 2021	Transoral	DFS	Bronchoscope	Y	in-vivo (3-D bronchus)	Static
[119] Huang 2021	Transanal	LRPA*	Colonoscope	Y	in-vitro (2-D colon)	Dynamic
[95] Wang 2021	Transnasal	CBS	Endoscope	N	in-silico (3-D nasal cavity)	Static
[118] Ravigopal 2021	Endovascular	Hybrid A*	Robotic guidewire	Y	in-vitro (2-D vessel)	Static
sampling-based:						
[126] Alterovitz 2011	Transoral	RRM	Concentric tube robot	Y	in-silico (3-D bronchus)	Static
[127] Torres 2011	Transnasal	RRM	Concentric tube robot	Y	in-silico (3-D nasal cavity)	Static
[128] Torres 2012	Transoral	RRM	Concentric tube robot	Y	in-silico (3-D bronchus)	Static
[129] Torres 2014	Transnasal	RRG	Concentric tube robot	Y	in-silico (3-D nasal cavity)	Static
[123] Fellmann 2015	Transnasal	RRT	Concentric tube robot	Y	in-silico (3-D nasal cavity)	Static
[124] Kuntz 2015	Transoral	RRT	Steerable needle	Y	in-silico (3-D bronchus)	Static
[121] Aguilar 2017	Transoral	bi-RRT	Bronchoscope	Y	in-silico (3-D bronchus)	Static
[122] Aguilar 2017	Transoral	bi-RRT	Bronchoscope	Y	in-silico (3-D bronchus)	Static
[131] Fauser 2018	Endovascular	bi-RRT	Catheter	Y	in-silico (3-D vena cava)	Static
[132] Fauser 2019a	Endovascular	bi-RRT	Steerable guidewire	Y	in-silico (3-D aorta)	Static
[133] Fauser 2019b	Endovascular	bi-RRT	Steerable guidewire	Y	in-silico (3-D aorta)	Static
[134] Kuntz 2019	Transnasal	PRM*	Concentric tube robot	Y	in-silico (3-D nasal cavity)	Dynamic
[125] Guo 2021	Endovascular	RRT	Catheter	N	in-silico (cerebrovascular)	Static
Optimisation-based:						
[135] Lyons 2010	Transoral endotracheal	Mathematical model	Concentric tube robot	Y	in-silico (3-D bronchus)	Static
[141] Gao 2015	Endovascular	ACO	Catheter	Y	in-silico (3-D lower limb arteries)	Static
[138] Qi 2019	Endovascular	Mathematical model	Continuum robot	Y	in-vitro (blood vessels)	Static
[142] Li 2021	Endovascular	GA	Catheter	Y	in-silico (3-D aorta and coronaries)	Static
[139] Guo 2021	Endovascular	Mathematical model	Catheter	Y	in-silico, in-vitro (3-D vessel model)	Static
[140] Abah 2021	Endovascular	Mathematical model	Catheter	Y	in-vitro (3-D cerebrovascular)	Static
Learning-based:						
[149] Zhao 2022	Endovascular	LfD using GAN	Guidewire	N	in-vitro (3-D vessel model)	Static
[154] Meng 2021	Endovascular	RL	Catheter	N	in-silico (3-D aorta)	Static
Level 2: Navigation using waypoints						
Learning-based:						
[150] Trovato 2010	Transanal	RL	Fibre optic endoscope	N	ex-vivo (3-D swine colon)	Dynamic
[144] Rafii-Tari 2013	Endovascular	LfD using GMM	Catheter	N	in-vitro (3-D aorta)	Static
[143] Rafii-Tari 2014	Endovascular	LfD using H+HMM	Catheter	Y	in-vitro (3-D aorta)	Static
[146] Chi 2018a	Endovascular	LfD using DMPs	Catheter	Y	in-vitro (3-D aorta)	Dynamic
[145] Chi 2018b	Endovascular	LfD using GMMs	Catheter	N	in-vitro (3-D aorta)	Static
[148] Chi 2020	Endovascular	LfD using GAIL	Catheter	N	in-vitro (3-D aorta)	Static
Level 3: Semi-autonomous navigation						
Node-based:						
[105] Qian 2019	Endovascular	Dijkstra	Guidewire	N	in-vitro (3-D femoral arteries, aorta)	Static
[112] Girerd 2020	Transnasal	Potential field	Concentric tube robot	Y	in-silico (3-D nasal cavity), in-vitro (origami tunnel)	Static
[110] Martin 2020	Transanal	Potential field	Endoscope	Y	in-vivo (3-D colon)	Dynamic
[111] Zhang 2020	Transanal	Potential field	Endoscope	Y	in-vitro (2-D colon model)	Dynamic
[107] Cho 2021	Endovascular	Dijkstra	Guidewire	N	in-vitro (2-D vessel)	Static
[99] Fischer 2022	Endovascular	BFS	Catheter	N	in-vitro (2-D vessel)	Static
[106] Schegg 2022	Endovascular	Dijkstra	Guidewire	N	in-silico (3-D coronary arteries)	Static
Learning-based:						
[28] You 2019	Endovascular	RL	Catheter	N	in-vitro (3-D heart)	Static
[152] Behr 2019	Endovascular	RL	Catheter	N	in-vitro (2-D vessel)	Static
[153] Karstensen 2020	Endovascular	RL	Catheter	N	in-vitro (2-D vessel)	Static
[156] Kweon 2021	Endovascular	RL	Guidewire	N	in-vitro (2-D coronary artery)	Static
[157] Pore 2022	Transanal	RL	Endoscope	N	in-silico (3-D colon)	Dynamic
[155] Karstensen 2022	Endovascular	RL	Guidewire	N	ex-vivo (2-D venous system)	Dynamic

path solution is not generated autonomously through a graph search strategy, especially when there are multiple path solutions simultaneously.

b) Depth first search: As an extended method to travel the tree formed in [67], the studies by Zang et al. [69], [96] implement a route search strategy of DFS for an integrated endobronchial ultrasound bronchoscope, exploring a graph by expanding the most promising node along the depth. In another study by Gibbs et al. [97], a DFS to view sites is regarded as the first phase search, followed by a second search focusing on

an ROI localization phase and a final refinement to adjust the viewing directions of the bronchoscope. A DFS approach is also developed in Huang et al. [98] for EI. Instead of considering path length as node weights in the typical DFS approach, this work defines the node weights as an experience value set by doctors.

The search time and the planned path are significantly dependent on the order of nodes in that same graph layer. Even though a DFS approach can search for a feasible path by first exploring the graph along with the depth, it does not ensure that the first path found is the optimal path.

c) Breadth first search: The BFS algorithm was employed in [99] for a magnetically actuated catheter to find a path reaching the target along vascular centerline points. However, the BFS algorithm would take much more time to find a solution in a complex vascular environment with multibranches.

d) Dijkstra: A graph structure based on vasculature's centerlines that are determined using a volume growing and a wavefront technique is designed by Schafer et al. in [100]. The optimal path is then determined using the shortest path algorithms from Dijkstra. However, Schafer et al. assumed that the centerline points are input as an ordered set, which would be a strict assumption. Moreover, they only report the scenario of a single lumen without branches, which does not reflect the advantages of the Dijkstra algorithm. A similar method but in a backward direction is presented by Egger et al. [101]. This work determines an initial path by Dijkstra. Users define initial and destination points. After that, the initial path is aligned with the blood vessel, resulting in the vasculature's centerline. However, this methodology is not fully autonomous, and it involves manually tuned parameters. Another work extracts the centerline and places a series of guiding circular workspaces along the navigation path that are perpendicular to the path [102]. The circular planes jointly form a safe cylindrical path from the start to the target. The Dijkstra algorithm is implemented to find the minimal cumulative cost set of voxels within the airway tree for bronchoscope navigation [103], [104] and find the shortest path along vasculature's centerlines [105], [106], [107].

Compared to DFS, Dijkstra keeps tracking and checking the cost until it reaches the target. So there is a higher possibility of getting a better solution. Nevertheless, these research works still focus on tracking anatomical centerlines that are difficult to follow precisely and often not desirable. Because aligning the instrument tip with the centerline may call for excessive forces at more proximal points along the instrument's body where contact with the anatomy occurs.

e) Potential field: The work by Rosell et al. [108] computed the potential field over grids based on the L1 distance to obstacles. It is used to search a path by wavefront propagation for bronchoscopy. Rosell's approach considers the geometry and kinematic constraints while selecting the best motion according to a cost function. Yang et al. [109] extract centerlines via a distance field method, establish and navigate the tree after that. However, the authors only considered the curvature constraint at 180° turns along vasculature's centerlines and assumed that all the path points have the same Y-coordinate. Martin et al. [110] employed a potential field approach by defining an attractive force from the endoluminal image center mass to the colon center mass. A linear translation between the colon center mass and the image center is reconstructed and regarded as the linear motion of the colonoscope tip. This work is validated both in the synthetic colon and pig colon (in-vivo). A similar approach is followed by Zhang et al. [111] where a robotic endoscope platform is employed to bring surgical instruments at the target site. Girerd et al. [112] used a 3-D point cloud representation of a tubular structure and compute a repulsive force to ensure that the concentric tube needle tip remains inside the contour.

The potential field has an advantage in local planning by maintaining the center of the image close to the center of the cross-section of the lumen or the vessels. Nevertheless, it only considers a short-term benefit rather than global optimality

during this local planning and might get stuck in a local minimum during global path planning.

f) A and LPA*:* He et al. [113] computed and optimized endoscopic paths using the A* algorithm. The effectiveness of the preoperatively planned path is verified by an automatic virtual nasal endoscopy browsing experiment. Ciobirca et al. [114] searched shortest airway paths through voxels of a bronchus model using the A* algorithm. They claimed that this method could potentially improve the diagnostic success rate with a system for tracking the bronchoscope during a real procedure. However, this statement has not been validated yet. Some studies proposed a path planning method for concentric tube robots (CTRs) in brain surgery. The authors of these studies build a nearest-neighbor graph and use LPA* algorithm for efficient replanning to optimize the insertion pose [115], [116]. Compared to A*, LPA* [117] can reuse information from previous searches to accelerate future ones. Ravigopal et al. [118] proposed a modified hybrid A* search algorithm to navigate a tendon-actuated coaxially aligned steerable guidewire robot along a precomputed path in 2-D vasculature phantoms under C-arm fluoroscopic guidance. Recently, Huang et al. [119] showed colon navigation using a real-time heuristic searching method, called learning real-time A* (LRTA*). LRTA* with designed directional heuristic evaluation shows efficient performance in colon exploration compared to BFS and DFS. Directional biasing avoids the need for unnecessary searches by constraining the next state based on local trends.

A* and LPA* use heuristic information to reach the goal. The first is commonly used for static environments, while the second can adapt to changes in the environment. They can converge very fast while ensuring optimality because both the cost from the start and the cost to the goal are taken into account. But their execution performance depends on the accuracy of the heuristic information. If inaccurate heuristic information is employed, searching in nonoptimal directions severely affects its performance.

g) Wall-following: The study in [120] uses a wall-following algorithm to assist catheter navigation. Fagogenis et al. [120] employed haptic vision to accomplish wall-following inside the blood-filled heart for a catheter. The wall-following algorithm could be considered an efficient navigation approach if there are few feasible routes to reach the target state. Otherwise, the solution of a wall-following algorithm cannot ensure optimality.

2) Sampling-Based Algorithms: As observable in Table III, different works, in the context of MP for IPEI, exploit sampling-based methods. As schematized in Fig. 6, algorithms based on rapidly exploring random tree (RRT) and its variants and probabilistic roadmap* (PRM*) have been proposed.

a) RRT and its variants: Some studies compare several RRT-based algorithms looking for the optimal option for the virtual bronchoscopy simulator, such as RRT, RRT-connect, dynamic-domain RRT, and RRT-connect with dynamic-domain [121], [122]. Results reveal that the RRT-connect with dynamic domain is the optimal method requiring the minimum number of samples and computational time for finding the solution path. Fellmann et al. [123] used a collision-free path via RRT as a baseline. Then different trajectory generation strategies are applied and evaluated. Inside the narrow and straight nasal passage, Fellmann et al. reported that the best

strategy is synchronous point-to-point. However, that strategy could become infeasible as the distance between intermediate configurations increases. Kuntz et al. [124] introduced an RRT-based algorithm in a three-step planning approach for a novel transoral lung system consisting of a bronchoscope, a CTR, and a bevel-tip needle. Their approach considers the ability of needle steering during path planning. Kuntz et al. demonstrated the motion planner's ability to respect a maximum needle steering curvature. The time to find a motion plan significantly depends on the steering capability and the target location.

The study in [125] implements an improved RRT algorithm for cerebrovascular intervention. The expansion direction of the random tree is a tradeoff between the new randomly sampled node and the target. This strategy can improve the convergence speed of the algorithm, even if catheter constraints are not considered.

Alterovitz et al. [126] proposed an RRM method that initially explores the configuration space, such as RRT. Once a path is found, RRM uses a user-specified parameter to weigh whether to explore further or to refine the explored space by adding edges to the current roadmap to find higher quality paths in the explored space. Their method is presented for CTRs in a tubular environment with protrusions as bronchus. Some studies develop the RRM method and improve it with more accurate mechanics-based models in a skull base surgery scenario and static lung bronchial tubes for CTRs, respectively [127], [128]. In Torres et al.'s work [127], the planner required 1077 s to get a motion plan that avoids bone, critical blood vessels, and healthy brain tissue on the way to the skull base tumour. The same authors extend the previous studies in [129] by proposing a modified RRG method that computes motion plans at interactive rates. This work improves the computation cost and allows replanning when the robot tip position changes. However, generating such a roadmap requires an extensive amount of computation. Therefore, the method could behave well in a static environment but not in deformable lumens.

Fauser et al. [130] used the formulation of RRT-connect (or bidirectional RRT, bi-RRT) introduced earlier by them to solve a common MP problem for instruments that follow curvature constrained trajectories [131]. In [132], Fauser et al. implemented the RRT-connect algorithm for a catheter in a 3-D static aorta model, under the allowed maximal curvature 0.1 mm^{-1}. Further extension of this work proposes path replanning from different robot position states along the initial path starting from the descending aorta to the goal in the left ventricle [133].

b) Probabilistic roadmap*: Kuntz et al. [134] proposed a method based on a combination of a PRM* method and local optimization to plan motions in a point cloud representation of a nasal cavity anatomy. The limitation is that the anatomy model is only updated within the visible region of the endoscope, while deformations of the rest of the anatomy are not considered. If tissue deformation is negligible, this planning method could be used for intraoperative planning. Otherwise, the deformations of the overall model must be considered beforehand.

3) Optimization-Based Algorithm: MP can be formulated as an optimization problem and solved by numerical solvers [85]. Moreover, these methods can be programmed to consider also the robotic kinematics.

a) Mathematical model: An optimization-based planning algorithm that optimizes the insertion length and orientation

angle of each tube for a CTR with five tubes is proposed by Lyons et al. [135]. First, the authors formulate the MP problem as a nonlinear constrained optimization problem. Second, the constraint is moved to the objective function, and the problem is converted to a series of unconstrained optimization problems. Finally, the optimal solution is found using the limited-memory Broyden–Fletcher–Goldfarb–Shanno algorithm [136] and Armijo's rule [137]. The robot kinematics is modeled using a physically based simulation that incorporates beam mechanics. This work is evaluated in simulation on a patient's lung anatomy. However, the computational time of the proposed method is high, which restricts the possibility of applying this method to real-time scenarios. Moreover, the authors manually define the skeleton and treat the structure as a rigid body, confining its applicability.

An inverse kinematics MP method for continuum robots is expressed as an optimization problem based on the backbone curve method by Qi et al. [138]. The technique minimizes the distance to the vasculature's centerline under kinematic constraints independently during each step without considering a long-term cumulative cost. Therefore, optimal inverse kinematics that does not consider the past and future phases might not be globally optimal.

Guo et al. [139] employed directional modeling of a teleoperated catheter and proposed a hybrid evaluation function to find the optimal trajectory. This work conducted wall-hit experiments and compared the response time of obstacle avoidance with and without path planning. However, the optimal solution is obtained with an exhaustive enumeration, which is a computationally expensive solution. Abah et al. [140] considered the path planning as a nonlinear least-squares problem to minimize the passive deflection of the steerable catheter. It is achieved by matching the shape of the steerable segment as closely as possible to the centerline of the cerebrovascular. Nevertheless, the centerline might not be the optimal reference route for steerable catheters.

b) Evolutionary algorithms: An improved ACO method is proposed to plan an optimal vascular path with overall consideration of factors, such as catheter diameter, vascular length, diameter, as well as curvature and torsion [141]. The associated computational time varied from 2 s to 30 s, with an average value 12.32 s. The high computational time cost limits its application in real-time scenarios. Li et al. [142] proposed a fast path planning approach under the steerable catheter curvature constraint via a local GA optimization. The reported results showed the planner's ability to satisfy the robot curvature constraint while keeping a low computational time cost of 0.191 ± 0.102 s.

4) Learning-Based Algorithms: Learning-based methods are a viable candidate for real-time MP. These methods use statistical tools, such as artificial neural networks, hidden Markov models (HMMs), and dynamical models to map perceptual and behavior spaces. In the context of this article, we identified learning from demonstrations (LfD) and reinforcement learning (RL) approaches as subfields of learning methods.

a) Learning from demonstrations: Rafii-Tari et al. [143] provided a system for human–robot collaboration for catheterization. The catheterization procedure is decomposed manually into a series of catheter movement primitives. These primitive motions are modeled as HMMs and are learnt using an LfD approach. In addition, a high-level HMM is learnt to sequence the motion primitives. Another system, proposed by the same authors, provides a semiautomated approach for

navigation, in which guidewire manipulation is controlled manually, and catheter motion is automated by the robot [144]. Catheter motion is modeled here using a Gaussian mixture model to create a representation of temporally aligned phase data generated from demonstrations. Chi et al. [145] extended this work by showing subject-specific variability among type I aortic arches through incorporating the anatomical information obtained from preoperative image data. In all the abovementioned methods, expectation maximization was used to perform maximum-likelihood estimation to learn the model parameters. Another study presents an LfD method based on dynamical movement primitives (DMPs) [146]. DMPs are compact representations for motion primitives formed by a set of dynamic system equations [147]. The study uses DMPs to avoid unwanted contact between the catheter tip and the vessel wall. DMPs were trained from human demonstrations and used to generate motion trajectories for the proposed robotic catheterization platform. The proposed methods can adapt to different flow simulations, vascular models, and catheterization tasks. In a recent continuation of their prior study, Chi et al. [148] improved the RL part by including model-free generative adversarial imitation learning loss that learns from multiple demonstrations of an expert. In this work, the catheterization policies adapt to the real-world setup and successfully imitate the task despite unknown simulated parameters, such as blood flow and tissue-tool interaction. Zhao et al. [149] proposed a generative adversarial network framework by combining convolutional neural network and long short-term memory to estimate suitable manipulation actions for catheterization. The deep neural network (DNN) is trained using experts' demonstration data and evaluated in a phantom with a gray-scale camera simulating X-ray imaging.

b) Reinforcement learning: Trovato et al. developed a hardware system for a robot colonic endoscope. It showed that the voltage for propulsion could be controlled through classic RL algorithms, such as state-action-reward-state-action and Q-learning that could determine the forward and backward motion [150]. Existing state-of-the-art RL algorithms use DNN to learn from high-dimensional and unstructured state inputs with minimal feature engineering to accomplish tasks, called deep reinforcement learning (DRL) [151]. Recently, Behr et al. [152], Karstensen et al. [153], and Meng et al. [154] proposed a closed-loop control system based on DRL, which uses the kinematic coordinates of the guidewire tip and manipulator as input and outputs continuous actions for each DoF for rotation and translation. Karstensen et al. [155] showed the translation in ex-vivo veins of a porcine liver. To improve the previously closed-loop control, You et al. [28] and Kweon et al. [156] automated control of the catheter using DRL based on image inputs in addition to the kinematic information of the catheter. The authors train a policy in a simulator and show its translation to a real robotic system. The real robotic experiments are carried out using the tip position from an electromagnetic sensor sent to the simulator to realize the virtual image input.

For transanal IP, Pore et al. [157] proposed a deep visuomotor control to map the endoscopic images to the control signal. The study reported efficient colon navigation in various in-silico colon models and better navigation performance compared to experts in terms of overall trajectory properties. Other efforts where some applications of DRL are emerging is tracheotomy. For

example, Athiniotis et al. [158] used a snake-like clinical robot to navigate down the airway autonomously. In this work, they employ a deep Q-network-based navigation policy that utilizes images from a monocular camera mounted on its tip. The system serves as an assistive device for medical personnel to perform endoscopic intubation with minimal human intervention.

C. Limitations of Present MP Methods

MP is a key ingredient in enabling autonomous navigation. However, it suffers some limitations that hinder their universal application in IPEI procedures. In this section, we identify the limitations of the aforementioned MP methods.

Node-based: The searching strategy of node-based algorithms is based on specific cost functions. The optimality and completeness of the solution obtained using this strategy could be guaranteed. However, i) node-based algorithms usually lack the consideration to satisfy robot capability during MP, such as robots' kinematic constraints; ii) the uncertainty of sensing is rarely considered; iii) the proposed methods are only applied in rigid environments, tissue deformations during procedures are not incorporated; iv) node-based algorithms usually rely on the thorough anatomical graph structures. Accurate reconstructions of the anatomical environment in the preoperative phase are needed to build the data structure and search inside it. The mentioned limitations reduce the usability of these methods. In theory, they may work, but in practice, they are difficult to be applied for autonomous real-time navigation in real-life conditions.

Sampling and optimization-based: Sampling and optimization-based approaches can account for the robot-specific characteristics. Nevertheless, the performance of these methods is affected significantly by the robot model. Moreover, especially for continuum soft robots, [2], the modeling methods and soft constraints of obstacle collision are challenging and still under investigation. Sampling-based approaches reduce computational time compared to optimization approaches but do not ensure the solution's optimality. The "probabilistic" completeness of sampling-based methods is their intrinsic property due to their random sampling. In other words, finding a feasible path solution is not always guaranteed. Existing optimization-based methods are time-consuming and mainly applied in static environments for preoperative MP. Hybrid methods that fuse multiple approaches could maximize their respective advantages.

Learning-based: Learning-based methods implemented in robotics have been rising. However, current challenges associated with learning-based methods limit their universal application in the clinical scenario [159]: One of the major concerns is safety [160]. Recently developed learning methods make use of DNN that can show unpredictable behavior for unseen data outside the training regime. Hence, ensuring that the DNN never makes decisions that can cause a safety violation is crucial [161], [162]. In addition, DNN-based learning methods require a huge amount of training data due to their inherent complexity, the large number of parameters involved and the learning optimization [163]. Therefore, a massive amount of data need to be acquired, moved, stored, annotated, and queried in an efficient way [164]. In the surgical domain, high-quality diverse

information is rarely available [48]. Various groups have proposed shared standards for device integration, data acquisition systems, and scalable infrastructure for data transmission, such as the connected optimized network and data in operating rooms project[1] and OR black box [165]. A general trend to overcome data limitations is through the use of simulators. However, it is challenging to generalize the knowledge gained through training in a simulator to a real situation, called the "sim-to-real" reality gap. Discrepancies between reality and virtual environment occur due to modeling errors [166]. Notably, model-free DRL is a widely popular way of learning goal-directed behaviors and has shown promising success in controlled robotic environments [159]. Some commonly used algorithms include PPO (on-policy) [167], SAC (off-policy) [168]. However, model-free DRL suffers from several limitations. First, there is a need to design a reward function implicitly. This need requires the developer to have domain knowledge of the dynamics of the environment [159], which is highly complex for deformable objects and tissues [169], [170]. Second, sensitivity to hyperparameters and underoptimized parameters can cause a significant difference in performance. Hence, a considerable amount of time has to be invested in tuning hyperparameters. Third, learning from high-dimensional inputs, such as images, is challenging compared to low-dimensional state features, such as robot kinematic data and has shown generalization problems due to the high capacity of DNN [159]. Fourth, continuum robots, such as endoscopes add to the dimensionality of the action space since they have a high number of DoFs with complex architectures, compared to industrial robots [171]. Some algorithm difficulty involves restricted policy search.

LfD is a preferred way to learn human gestures in the context of imitation learning [172]. However, a significant drawback of LfD methods is that they require many demonstrations to be adequately trained, which is unfeasible in clinical settings considering the time, resources, and ethical constraints. Furthermore, LfD typically only enables the robot to become as good as the human's demonstrations since a large deviation of the policy from the demonstrated data could lead to unstable policy learning [173].

V. Future Directions

Navigation is one of the crucial interventional phases of an IPEI procedure. The need for automation in IPEI navigation will increasingly support the adoption of novel MP techniques capable of working in unstructured and dynamic luminal environments. In this section, we describe the improvements in MP algorithms that have been applied in other robotics domains and can be extended to IPEI. Moreover, robot navigation relies on robot design and its sensing capabilities. Therefore, we discuss the essential robotics capabilities still missing to enable navigation systems with a higher level of autonomy (e.g., LoA 4).

A. Improvements in MP Algorithms

MP for continuum robots is a complex problem because many configurations exist with multiple internal DoFs that have to be coordinated to achieve purposeful motion [16], [171], 32 of 65 publications consider MP for the robot without considering its

kinematics, as shown in Table III. Future studies need to focus on the robotic constraints for active MP. Moreover, replanning is required to adapt the current plan to deformable environments using sensorial information. The objective of replanning is to reduce the navigation error measured according to defined metrics. Therefore, the computational efficiency of MP becomes essential for real-time scenarios. This section highlights insights that can improve existing MP techniques, as discussed in Section IV.

Some novel studies on the path planning of a steerable needle for neurosurgery could give some inspiration for IPEI, as these studies considered curvature constraints of a robotic needle. Parallel path exploration is used in the adaptive fractal trees (AFT) proposed for a programmable bevel-tip steerable needle [174]. This method uses fractal theory and graphics processing units (GPUs) architecture to parallelize the planning process, and enhance the computation performance and online replanning, as demonstrated with simulated 3-D liver needle insertions. An adaptive hermite fractal tree (AHFT) is later proposed, where the AFT is combined with optimized geometric hermite curves that allow performing a path planning strategy satisfying the heading and targeting curvature constraints [175]. Although developed and tested only for a preoperative neurosurgical scenario, AHFT is well-suited for GPU parallelization for rapid replanning.

Hybrid approaches can take advantage of individual methods to show enhanced performance and overcome the limitation of each method. The emerging learning-based approaches can be combined with other methods to overcome their limitations. For example, Wang et al. [176] proposed a hybrid approach combining RL and RRT algorithms for MP in narrow passages. Their method can enhance the local space exploration ability and guarantee the efficiency of global path planning. Some other authors also present hybrid MP methods for IPEI navigation. For example, Meng et al. [74] proposed a hybrid method using BFS and GA for microrobot navigation in blood vessels of rat liver, aiming to minimize the energy consumption.

Optimization-based methods are also an active area of research for obtaining an optimal preoperative plan under complex constraints. Particle swarm optimization is implemented by Granna et al. [177] for a concentric tube robotic system in neurosurgery. Dynamic programming is employed for microrobot path planning in rigid arteries under a minimum effort criterion [178]. However, the search space reduction technique for the constrained optimization problem is essential for intraoperative MP. Howell et al. [179] proposed an augmented Lagrangian trajectory optimizer solver for constrained trajectory optimization problems. It handles general nonlinear state and input constraints and offers fast convergence and numerical robustness. For an IPEI motion planner, an efficient optimization solver with reduced search space would be potentially applied for intraoperative planning.

As demonstrated in Fig. 7, the recent shift toward learning-based approaches has shown promising success. The guarantee of a provable behaviors using DNN is still an open problem, and it is crucial to incorporate safety constraints for the automation of IPEI navigation tasks to avoid hazardous actions. Some studies have proposed safe RL frameworks for safety-critical paradigms using barrier functions to restrict the robot actuation in a safe workspace [160], [180] and its behaviors is formally verified to guarantee safety [161], [162]. Robot unsafe behavior can also be generated due to large policy updates of gradient-based

[1][Online]. Available: https://condor-h2020.eu/

optimisation. Such large deviations can be limited by restricting the policy update in a trust region, leading to monotonic improvement in policy performance. Some works use f-divergences methods, such as KL-divergence, to constrain the policy search from being greedy [167]. To tackle the problem of high cost and danger of interacting with the environment and data inefficiency of existing DRL methods, recent studies have explored offline RL that learns exclusively from static datasets of previously collected experiences [181].

Commonly used model-free RL techniques do not consider the dynamics of the environment [182]. However, various complexities, such as pulsatile flow within the vasculature or nonlinear behavior of the instrument, hinder the implementation of model-free algorithms and compel to simplify the problem sets. Thus, the future trend could involve implementing model-based approaches in endoluminal or endovascular environments [183]. Model-based approaches are sample efficient and require less data for training [184]. Hierarchical RL is another untapped field for long navigation tasks, which is oriented to subdivide the interventional phase into steps and applying specific policies to each. This approach better adapts to the specifications of each phase. For example, in the case of IPEI navigation, the complete navigation task could be subdivided and learnt incrementally [185]. Recently, curriculum learning has been proposed to learn in increasingly complex environments [186].

B. Robotic Capabilities

Reaching higher LoA in navigation requires accurate control and enhanced shape-sensing capabilities. In this section, we discuss various missing capabilities in current IPEI robotic systems that hinder the development of an LoA 4 navigation system.

1) Robotics Actuation: Continuum robots employed in IPEI procedures are developed based on different designs and technologies. For instance, several continuum instruments use concentric tube mechanisms or multilink systems [15], [16]. Soft-robotics systems are an emerging paradigm that can enable multisteering capabilities and complex stress-less interventions through narrow passageways. IPEI scenarios reflect an environment where the snake-like robot can use the wall as a support to propel forward. Bioinspired robots imitate biological systems, such as snake locomotion [187], [188], octopus tentacles [189], elephant trunks [190], and mammalian spine [191]. They have been an emerging research direction in soft-robotic actuation [192]. Pressure-driven eversion of flexible, thin-walled tubes, called vine robots, has shown increased applications to navigate confined spaces [193].

2) Proprioception and Shape Sensing: To achieve precise and reliable motion control of continuum robots, accurate and real-time shape sensing is needed. However, accurately modeling the robot shape is challenging due to friction, backlash, the inherent deformable nature of the lumen or vessels and inevitable collisions with the anatomy [194]. Some emerging sensor-based shape reconstruction techniques for interventional devices rely on fiber Bragg Gratings (FBG) and electromagnetic (EM) sensors [194], [195], [196], [197], [198]. Both FBG and EM enabled techniques provide real-time shape estimation due to their short response time, miniature size, biocompatibility, nontoxicity, and high sensitivity. Multiple sensors can be attached along the

length of the continuum robot to track the robot and measure the axial strain. However, FBG sensors provide a poor response in high-strain conditions and EM sensors suffer from the problem of EM interference [195]. Hence, a sensor-fusion method between FBG, EM sensors, and sparse fluoroscopic images could improve 3-D catheter shape reconstruction accuracy [198].

3) Lumen/vessel Modeling: Intraoperative imaging modalities, such as ultrasound and optical coherence tomography can support direct observation and visualization [199], [200], [201]. Sensor fusion between intravascular ultrasound and EM can provide an intravascular reconstruction of vessels [199], [202]. For computer-assisted navigation, simultaneous localization and mapping has been successfully demonstrated in inferring dense and detailed depth maps and lumen reconstruction [203]. Depth prediction models have been developed recently to estimate lumen features [204].

VI. Conclusion

Navigation is one of the crucial steps of IPEI that requires extensive interventional dexterity and skills. This work provides a detailed overview of several critical aspects required to improve IPEI navigation. We propose a classification of dedicated autonomy levels and provide a systematic review of the governing motion planning methods. Autonomous navigation could improve the overall execution of IPEI procedures, enabling the interventionist to focus on the medical aspects rather than on control issues with the instruments. Therefore, in this article, we define the LoA required for IPEI navigation and the foreseeable human intervention associated with each level. This classification will improve risk and safety management while we advance toward higher LoA. One of the essential steps toward achieving automation is through employing MP methods. A comprehensive overview of MP techniques used in IPEI navigation is provided in this work. At the same time, the limitations associated with existing methods are provided. These voids in capabilities need to be overcome if one wants to raise the level of autonomy of today's existing robotic systems. These include improvements in MP techniques and in enhanced robotic capabilities, such as actuation and proprioception modeling. Autonomous navigation can positively impact IPEI procedures, making them widely accessible to a greater population.

References

[1] J. Seetohul et al., "Snake robots for surgical applications: A review," *Robot.*, vol. 11, no. 3, p. 57, 2022.

[2] T. da Veiga et al., "Challenges of continuum robots in clinical context: A review," *Prog. Biomed. Eng.*, vol. 2, no. 3, 2020, Art. no. 032003.

[3] N. Simaan et al., "Medical technologies and challenges of robot-assisted minimally invasive intervention and diagnostics," *Annu. Rev. Control Robot. Auton. Syst.*, vol. 1, pp. 465–490, 2018.

[4] J. M. Prendergast, G. A. Formosa, C. R. Heckman, and M. E. Rentschler, "Autonomous localization, navigation and haustral fold detection for robotic endoscopy," in *Proc. IEEE/RSJ Int. Conf. Intell. Robot. Syst.*, 2018, pp. 783–790.

[5] J. Hwang et al., "A review of magnetic actuation systems and magnetically actuated guidewire-and catheter-based microrobots for vascular interventions," *Intell. Serv. Robot.*, vol. 13, no. 1, pp. 1–14, 2020.

[6] A. Orekhov et al., "Snake-like robots for minimally invasive, single-port, and intraluminal surgeries," *Encyclopedia Med. Robot. World Sci.*, pp. 203–243, 2018.

[7] L. Manfredi, "Endorobots for colonoscopy: Design challenges and available technologies," *Front. Robot. AI*, vol. 8, 2021, Art. no. 705454.

[8] P. Fiorini, K. Y. Goldberg, Y. Liu, and R. H. Taylor, "Concepts and trends in autonomy for robot-assisted surgery," *Proc. IEEE*, vol. 110, no. 7, pp. 993–1011, Jul. 2022.

[9] A. Attanasio et al., "Autonomy in surgical robotics," *Annu. Rev. Control Robot. Auton. Syst.*, vol. 4, pp. 651–679, 2020.

[10] T. Haidegger, "Autonomy for surgical robots: Concepts and paradigms," *IEEE Trans. Med. Robot. Bionics*, vol. 1, no. 2, pp. 65–76, May 2019.

[11] R. Hargest, "Five thousand years of minimal access surgery: 1990–present: Organisational issues and the rise of the robots," *J. Roy. Soc. Med.*, vol. 114, no. 2, pp. 69–76, 2021.

[12] G.-Z. Yang et al., "Medical robotics–regulatory, ethical, and legal considerations for increasing levels of autonomy," *Sci. Robot.*, vol. 2, no. 4, 2017, Art. no. 8638.

[13] B. Patle et al., "A review: On path planning strategies for navigation of mobile robot," *Defence Technol.*, vol. 15, no. 4, pp. 582–606, 2019.

[14] J.-C. Latombe, *Robot Motion Planning*. Berlin, Germany: Springer, 2012, vol. 124.

[15] O. M. Omisore, S. Han, J. Xiong, H. Li, Z. Li, and L. Wang, "A review on flexible robotic systems for minimally invasive surgery," *IEEE Trans. Syst., Man, Cybern.: Syst.*, vol. 52, no. 1, pp. 631–644, Jan. 2022.

[16] J. Burgner-Kahrs, D. C. Rucker, and H. Choset, "Continuum robots for medical applications: A survey," *IEEE Trans. Robot.*, vol. 31, no. 6, pp. 1261–1280, Dec. 2015.

[17] V. Vitiello, S. -L. Lee, T. P. Cundy, and G.-Z. Yang, "Emerging robotic platforms for minimally invasive surgery," *IEEE Rev. Biomed. Eng.*, vol. 6, pp. 111–126, 2013.

[18] M. Blecha et al., "Modern endovascular therapy," *World J. Surg.*, vol. 45, pp. 3493–3502, 2021.

[19] A. B. Villaret et al., "Robotic transnasal endoscopic skull base surgery: Systematic review of the literature and report of a novel prototype for a hybrid system (Brescia endoscope assistant robotic holder)," *World Neurosurgery*, vol. 105, pp. 875–883, 2017.

[20] B. S. Peters et al., "Review of emerging surgical robotic technology," *Surg. Endoscopy*, vol. 32, no. 4, pp. 1636–1655, 2018.

[21] H. Rafii-Tari et al., "Current and emerging robot-assisted endovascular catheterization technologies: A review," *Ann. Biomed. Eng.*, vol. 42, no. 4, pp. 697–715, 2014.

[22] J. Bonatti et al., "Robotic technology in cardiovascular medicine," *Nature Rev. Cardiol.*, vol. 11, no. 5, 2014, Art. no. 266.

[23] Y. Fu et al., "Steerable catheters in minimally invasive vascular surgery," *Int. J. Med. Robot. Comput. Assist. Surg.*, vol. 5, no. 4, pp. 381–391, 2009.

[24] A. Pourdjabbar et al., "The development of robotic technology in cardiac and vascular interventions," *Rambam Maimonides Med. J.*, vol. 8, no. 3, 2017.

[25] M. Berczeli et al., "Catheter robots in the cardiovascular system," *Latest Develop. Med. Robot. Syst.*, pp. 95–106, 2021.

[26] G. Ciuti et al., "Frontiers of robotic colonoscopy: A comprehensive review of robotic colonoscopes and technologies," *J. Clin. Med.*, vol. 9, no. 6, 2020, Art. no. 1648.

[27] C.-K. Yeung et al., "Emerging next-generation robotic colonoscopy systems towards painless colonoscopy," *J. Dig. Dis.*, vol. 20, no. 4, pp. 196–205, 2019.

[28] H. You et al., "Automatic control of cardiac ablation catheter with deep reinforcement learning method," *J. Mech. Sci. Tech.*, vol. 33, no. 11, pp. 5415–5423, 2019.

[29] M. Lemke et al., "Colonoscopy trainers experience greater stress during insertion than withdrawal: Implications for endoscopic curricula," *J. Can. Assoc. Gastroenterol.*, vol. 4, no. 1, pp. 15–20, 2021.

[30] R. Ahmed et al., "Colonoscopy technologies for diagnostics and drug delivery," *Med. Devices Sensors*, vol. 2, no. 3/4, 2019, Art. no. e10041.

[31] K. J. Wernli et al., "Risks associated with anesthesia services during colonoscopy," *Gastroenterology*, vol. 150, no. 4, pp. 888–894, 2016.

[32] C. Hassan et al., "Diagnostic yield and miss rate of endorings in an organized colorectal cancer screening program: The smart (study methodology for adr-related technology) trial," *Gastrointestinal Endoscopy*, vol. 89, no. 3, pp. 583–590, 2019.

[33] M. Than et al., "Diagnostic miss rate for colorectal cancer: An audit," *Ann. Gastroenterol.*, vol. 28, no. 1, pp. 94–98, 2015.

[34] A. Eickhoff et al., "In vitro evaluation of forces exerted by a new computer-assisted colonoscope (the neoguide endoscopy system)," *Endoscopy*, vol. 38, no. 12, pp. 1224–1229, 2006.

[35] N. Gluck et al., "A novel self-propelled disposable colonoscope is effective for colonoscopy in humans (with video)," *Gastrointestinal Endoscopy*, vol. 83, no. 5, pp. 998–1004, 2016.

[36] M. Shike et al., "Sightline colonosight system for a disposable, power-assisted, non-fiber-optic colonoscopy (with video)," *Gastrointestinal Endoscopy*, vol. 68, no. 4, pp. 701–710, 2008.

[37] E. Tumino et al., "Use of robotic colonoscopy in patients with previous incomplete colonoscopy," *Eur. Rev. Med. Pharmacol Sci.*, vol. 21, no. 4, pp. 819–826, 2017.

[38] S. D. Herrell et al., "Future robotic platforms in urologic surgery: Recent developments," *Curr. Opin. Urol.*, vol. 24, no. 1, pp. 118–126, 2014.

[39] M. D. Tyson et al., "Urological applications of natural orifice transluminal endoscopic surgery," *Nature Rev. Urol.*, vol. 11, no. 6, pp. 324–332, 2014.

[40] W. M. Bazzi et al., "Natural orifice transluminal endoscopic surgery in urology: Review of the world literature," *Urol. Ann.*, vol. 4, no. 1, pp. 3279–3286, 2012.

[41] Y. Chen et al., "Review of surgical robotic systems for keyhole and endoscopic procedures: State of the art and perspectives," *Front. Med.*, vol. 14, no. 4, pp. 382–403, 2020.

[42] J. Rassweiler et al., "Robot-assisted flexible ureteroscopy: An update," *Urolithiasis*, vol. 46, no. 1, pp. 69–77, 2018.

[43] G. Gandaglia et al., "Novel technologies in urologic surgery: A rapidly changing scenario," *Curr. Urol. Rep.*, vol. 17, no. 3, pp. 1–8, 2016.

[44] P. Valdastri et al., "Advanced technologies for gastrointestinal endoscopy," *Ann. Rev. Biomed. Eng.*, vol. 14, pp. 397–429, 2012.

[45] W. Marlicz et al., "Frontiers of robotic gastroscopy: A comprehensive review of robotic gastroscopes and technologies," *Cancers*, vol. 12, no. 10, 2020, Art. no. 2775.

[46] A. De Virgilio et al., "Trans-oral robotic surgery in the management of parapharyngeal space tumors: A systematic review," *Oral Oncol.*, vol. 103, 2020, Art. no. 104581.

[47] U. B. Prakash et al., "Bronchoscopy," *J. Bronchol. Interv. Pulmonol.*, vol. 1, no. 4, 1994, Art. no. 340.

[48] L. R. Kennedy-Metz et al., "Computer vision in the operating room: Opportunities and caveats," *IEEE Trans. Med. Robot. Bionics*, vol. 3, no. 1, pp. 2–10, Feb. 2021.

[49] A. Agrawal et al., "Robotic bronchoscopy for pulmonary lesions: A review of existing technologies and clinical data," *J. Thoracic Dis.*, vol. 12, no. 6, 2020, Art. no. 3279.

[50] H. Stammberger et al., "Functional endoscopic sinus surgery," *Eur. Arch. Oto-Rhino- Laryngol.*, vol. 247, no. 2, pp. 63–76, 1990.

[51] J. Burgner et al., "A telerobotic system for transnasal surgery," *IEEE Trans. Mechatronics*, vol. 19, no. 3, pp. 996–1006, Jun. 2014.

[52] A. Madoglio et al., "Robotics in endoscopic transnasal skull base surgery: Literature review and personal experience," *Control Syst. Des. Bio-Robot. Bio-Mechatronics With Adv. Appl.*, pp. 221–244, 2020.

[53] T. Tanuma et al., "Current status of transnasal endoscopy worldwide using ultrathin videoscope for upper gastrointestinal tract," *Dig. Endoscopy*, vol. 28, pp. 25–31, 2016.

[54] N. Simaan et al., "Design and integration of a telerobotic system for minimally invasive surgery of the throat," *Int. J. Robot. Res.*, vol. 28, no. 9, pp. 1134–1153, 2009.

[55] S. Y. Nof, "Automation: What it Means to us Around the World," in *Springer Handbook Automation*. Berlin, Germany: Springer, 2009, pp. 13–52.

[56] J. I. Olszewska et al., "Ontology for autonomous robotics," in *Proc. IEEE Int. Symp. Robot. Hum. Interact. Commun.*, 2017, pp. 189–194.

[57] H. Chen et al., "From automation system to autonomous system: An architecture perspective," *J. Mar. Sci. Eng.*, vol. 9, no. 6, 2021, Art. no. 645.

[58] M. Fisher et al., "Towards a framework for certification of reliable autonomous systems," *Auton. Agents Multi-Agent Syst.*, vol. 35, no. 1, pp. 1–65, 2021.

[59] F. Merenda et al., "Ethics, safety and human centricity: Intelligent machines under the scope of the European AI regulation act," in *Proc. Workshop Conf. Italian Inst. Robot. Intell. Mach.*, 2021.

[60] S. O'sullivan et al., "Legal, regulatory, and ethical frameworks for development of standards in artificial intelligence (AI) and autonomous robotic surgery," *Int. J. Med. Robot. Comput. Assist. Surg.*, vol. 15, no. 1, 2019, Art. no. e1968.

[61] E. Parliament and C. of the European Union, "Artificial intelligence act: Regulation laying down harmonised rules on artificial intelligence and amending certain union legislative acts," *Proposal for Regulation COM/2021/206*, 2021. [Online]. Available: https://eur-lex.europa.eu/legal-content/EN/TXT/?uri=celex%3A52021PC0206

[62] "National artificial intelligence initiative," [Online]. Available: https://www.congress.gov/bill/116th-congress/house-bill/6216/text

[63] M.-C. Fiazza, "The EU proposal for regulating AI: Foreseeable impact on medical robotics," in *Proc. IEEE Int. Conf. Adv. Robot.*, 2021, pp. 222–227.

[64] I. E. C. (2017c), "IEC TR 60601-4-1–medical electrical equipment – Part 4-1: Guidance and interpretation - medical electrical equipment and medical electrical systems employing a degree of autonomy," 2017. [Online]. Available: https://webstore.iec.ch/ publication/29312

[65] D. Katić et al., "Lapontospm: An ontology for laparoscopic surgeries and its application to surgical phase recognition," *Int. J. Comput. Assist. Radiol. Surg.*, vol. 10, no. 9, pp. 1427–1434, 2015.

[66] S. R. Ravigopal, T. A. Brumfiel, A. Sarma, and J. P. Desai, "Fluoroscopic image-based 3-D environment reconstruction and automated path planning for a robotically steerable guidewire," *IEEE Robot. Automat. Lett.*, vol. 7, no. 4, pp. 11918–11925, Oct. 2022.

[67] R. Khare, R. Bascom, and W. E. Higgins, "Hands-free system for bronchoscopy planning and guidance," *IEEE Trans. Biomed. Eng.*, vol. 62, no. 12, pp. 2794–2811, Dec. 2015.

[68] J.-Q. Zheng, X.-Y. Zhou, C. Riga, and G.-Z. Yang, "Towards path planning from a single 2D fluoroscopic image for robot assisted fenestrated endovascular aortic repair," in *Proc. IEEE Int. Conf. Robot. Automat.*, 2019, pp. 8747–8753.

[69] X. Zang et al., "Optimal route planning for image-guided EBUS bronchoscopy," *Comput. Biol. Med.*, vol. 112, 2019, Art. no. 103361.

[70] A. Z. Taddese et al., "Enhanced real-time pose estimation for closed-loop robotic manipulation of magnetically actuated capsule endoscopes," *Int. J. Robot. Res.*, vol. 37, no. 8, pp. 890–911, 2018.

[71] M. J. Page et al., "The prisma 2020 statement: An updated guideline for reporting systematic reviews," *Brit. Med. J.*, vol. 372, 2021, Art. no. 105906.

[72] M. E. Rose et al., "pybliometrics: Scriptable bibliometrics using a python interface to scopus," *SoftwareX*, vol. 10, 2019, Art. no. 100263.

[73] F. E. Vuik et al., "Colon capsule endoscopy in colorectal cancer screening: A systematic review," *Endoscopy*, vol. 53, no. 8, pp. 815–824, 2021.

[74] K. Meng, Y. Jia, H. Yang, F. Niu, Y. Wang, and D. Sun, "Motion planning and robust control for the endovascular navigation of a microrobot," *IEEE Trans. Ind. Inform.*, vol. 16, no. 7, pp. 4557–4566, Jul. 2020.

[75] B. Siciliano et al., *Springer Handbook of Robotics*, vol. 200. Berlin, Germany: Springer, 2008.

[76] L. Yang et al., "Survey of robot 3D path planning algorithms," *J. Control Sci. Eng.*, vol. 2016, 2016, Art. no. 7426913.

[77] R. Tarjan, "Depth-first search and linear graph algorithms," *SIAM J. Comput.*, vol. 1, no. 2, pp. 146–160, 1972.

[78] R. Dechter et al., "Generalized best-first search strategies and the optimality of A," *J. ACM*, vol. 32, no. 3, pp. 505–536, 1985.

[79] E. W. Dijkstra, "A note on two problems in connexion with graphs," *Numerische Mathematik*, vol. 1, no. 1, pp. 269–271, 1959.

[80] Y. K. Hwang and N. Ahuja, "A potential field approach to path planning," *IEEE Trans. Robot. Automat.*, vol. 8, no. 1, pp. 23–32, Feb. 1992.

[81] P. E. Hart, N. J. Nilsson, and B. Raphael, "A formal basis for the heuristic determination of minimum cost paths," *IEEE Trans. Syst. Sci. Cybern.*, vol. 4, no. 2, pp. 100–107, Jul. 1968.

[82] S. M. LaValle et al., "Rapidly-exploring random trees: A new tool for path planning," *Comput. Sci. Dept. Oct.*, vol. 98, no. 11, pp. 1–4, 1998.

[83] R. Geraerts et al., "A comparative study of probabilistic roadmap planners," in *Proc. Algorithmic Found. Robot.*, 2004, pp. 43–57.

[84] S. Karaman et al., "Sampling-based algorithms for optimal motion planning," *Int. J. Robot. Res.*, vol. 30, no. 7, pp. 846–894, 2011.

[85] P. Raja et al., "Optimal path planning of mobile robots: A review," *Int. J. Phys. Sci.*, vol. 7, no. 9, pp. 1314–1320, 2012.

[86] M. Dorigo, M. Birattari, and T. Stutzle, "Ant colony optimization," *IEEE Comput. Intell. Mag.*, vol. 1, no. 4, pp. 28–39, Nov. 2006.

[87] J. H. Holland et al., *Adaptation in Natural and Artificial Systems: An Introductory Analysis With Applications to Biology, Control, and Artificial Intelligence*. Cambridge, MA, USA: MIT Press, 1992.

[88] H. Ravichandar et al., "Recent advances in robot learning from demonstration," *Annu. Rev. Control, Robot., Auton. Syst.*, vol. 3, pp. 297–330, 2020.

[89] R. S. Sutton et al., *Reinforcement Learning: An Introduction*. Cambridge, MA, USA: MIT Press, 2018.

[90] B. Geiger, A. P. Kiraly, D. P. Naidich, and C. L. Novak, "Virtual bronchoscopy of peripheral nodules using arteries as surrogate pathways," in *Proc. Med. Imag.: Physiol. Func. Struct. from Med. Imag.*, 2005, vol. 5746, pp. 352–360.

[91] C. Sánchez et al., "Navigation path retrieval from videobronchoscopy using bronchial branches," in *Proc. Workshop Clin. Image. Based Procedures*, 2016, pp. 62–70.

[92] J. Wang et al., "Intravascular catheter navigation using path planning and virtual visual feedback for oral cancer treatment," *Int. J. Med. Robot. Comput. Assist. Surg.*, vol. 7, no. 2, pp. 214–224, 2011.

[93] F. Yang, Z.-G. Hou, S.-H. Mi, Gui-Bin Bian, and X.-L. Xie, "Centerlines extraction for lumen model of human vasculature for computer-aided simulation of intravascular procedures," in *Proc. IEEE World Congr. Intell. Control Automat.*, 2014, pp. 970–975.

[94] M. Kerschnitzki et al., "Architecture of the osteocyte network correlates with bone material quality," *J. Bone Mineral Res.*, vol. 28, no. 8, pp. 1837–1845, 2013.

[95] W. Yudong et al., "Rapid path extraction and three-dimensional roaming of the virtual endonasal endoscope," *Chin. J. Electron.*, vol. 30, no. 3, pp. 397–405, 2021.

[96] X. Zang et al., "Image-guided EBUS bronchoscopy system for lung-cancer staging," *Inform. Med. Unlocked*, vol. 25, 2021, Art. no. 100665.

[97] J. D. Gibbs, M. W. Graham, R. Bascom, D. C. Cornish, R. Khare, and W. E. Higgins, "Optimal procedure planning and guidance system for peripheral bronchoscopy," *IEEE Trans. Biomed. Eng.*, vol. 61, no. 3, pp. 638–657, Mar. 2014.

[98] D. Huang, W. Tang, Y. Ding, T. Wan, and Y. Chen, "An interactive preoperative planning and training system for minimally invasive vascular surgery," in *Proc. IEEE 12th Int. Conf. Comput. Aided Des. Comput. Graph.*, 2011, pp. 443–449.

[99] C. Fischer, Q. Boehler, and B. J. Nelson, "Using magnetic fields to navigate and simultaneously localize catheters in endoluminal environments," *IEEE Robot. Automat. Lett.*, vol. 7, no. 3, pp. 7217–7223, Jul. 2022.

[100] S. Schafer et al., "Planning image-guided endovascular interventions: Guidewire simulation using shortest path algorithms," in *Proc. Med. Imag.: Visual. Imag. Guid. Procedures*, 2007, vol. 6509, pp. 813–822.

[101] J. Egger, Z. Mostarkic, S. Grosskopf, and B. Freisleben, "A fast vessel centerline extraction algorithm for catheter simulation," in *Proc. 20th IEEE Int. Symp. Comput. Based Med. Syst.*, 2007, pp. 177–182.

[102] H. Liu et al., "An in vitro investigation of image-guided steerable catheter navigation," *Proc. Inst. Mech. Eng.: J. Eng. Med.*, vol. 224, no. 8, pp. 945–954, 2010.

[103] J. D. Gibbs et al., "path planning and extension for endoscopic guidance," in *Proc. Med. Imag.: Visual. Imag. Guid. Procedures*, 2007, pp. 554–566.

[104] J. D. Gibbs et al., "Integrated system for planning peripheral bronchoscopic procedures," in *Proc. Med. Imag.: Physiol. Func. Struct. Med. Imag.*, 2008, pp. 154–168.

[105] H. Qian et al., "Towards rebuild the interventionist's intra-operative natural behavior: A fully sensorized endovascular robotic system design," in *Proc. IEEE Int. Conf. Med. Imag. Phys. Eng.*, 2019, pp. 1–7.

[106] P. Schegg et al., "Automated planning for robotic guidewire navigation in the coronary arteries," in *Proc. IEEE 5th Int. Conf. Soft Robot.*, 2022, pp. 239–246.

[107] Y. Cho, J.-H. Park, J. Choi, and D. E. Chang, "Image processing based autonomous guidewire navigation in percutaneous coronary intervention," in *Proc. IEEE Int. Conf. Consum. Electron. Asia*, 2021, pp. 1–6.

[108] J. Rosell, A. Pérez, P. Cabras, and A. Rosell, "Motion planning for the virtual bronchoscopy," in *Proc. IEEE Int. Conf. Robot. Automat.*, 2012, pp. 2932–2937.

[109] F. Yang et al., "Path planning of flexible ureteroscope based on CT image," in *Proc. IEEE Chin. Control Conf.*, 2019, pp. 4667–4672.

[110] J. W. Martin et al., "Enabling the future of colonoscopy with intelligent and autonomous magnetic manipulation," *Nature Mach. Intell.*, vol. 2, no. 10, pp. 595–606, 2020.

[111] Q. Zhang, J. M. Prendergast, G. A. Formosa, M. J. Fulton, and M. E. Rentschler, "Enabling autonomous colonoscopy intervention using a robotic endoscope platform," *IEEE Trans. Biomed. Eng.*, vol. 68, no. 6, pp. 1957–1968, Jun. 2021.

[112] C. Girerd, A. V. Kudryavtsev, P. Rougeot, P. Renaud, K. Rabenorosoa, and B. Tamadazte, "SLAM-based follow-the-leader deployment of concentric tube robots," *IEEE Robot. Automat. Lett.*, vol. 5, no. 2, pp. 548–555, Apr. 2020.

[113] Y. He, P. Zhang, X. Qi, B. Zhao, S. Li, and Y. Hu, "Endoscopic path planning in robot-assisted endoscopic nasal surgery," *IEEE Access*, vol. 8, pp. 17039–17048, 2020.

[114] C. Ciobirca et al., "A new procedure for automatic path planning in bronchoscopy," *Mater. Today: Proc.*, vol. 5, no. 13, pp. 26513–26518, 2018.

[115] S. Niyaz et al., "Following surgical trajectories with concentric tube robots via nearest-neighbor graphs," in *Proc. Int. Symp. Exp. Robot.*, 2018, pp. 3–13.

[116] S. Niyaz, A. Kuntz, O. Salzman, R. Alterovitz, and S. S. Srinivasa, "Optimizing motion-planning problem setup via bounded evaluation with application to following surgical trajectories," in *Proc. IEEE/RSJ Int. Conf. Intell. Robot. Syst.*, 2019, pp. 1355–1362.

[117] N. Koenig and A. Howard, "Design and use paradigms for Gazebo, an open-source multi-robot simulator," in *Proc. IEEE/RSJ Int. Conf. Intell. Robot. Syst.*, 2004, vol. 3, pp. 2149–2154.

[118] S. R. Ravigopal, T. A. Brumfiel, and J. P. Desai, "Automated motion control of the coast robotic guidewire under fluoroscopic guidance," in *Proc. Int. Symp. Med. Robot.*, 2021, pp. 1–7.

[119] H.-E. Huang et al., "Autonomous navigation of a magnetic colonoscope using force sensing and a heuristic search algorithm," *Sci. Rep.*, vol. 11, no. 1, pp. 1–15, 2021.

[120] G. Fagogenis et al., "Autonomous robotic intracardiac catheter navigation using haptic vision," *Sci. Robot.*, vol. 4, no. 29, 2019, Art. no. eaaw1977.

[121] W. G. Aguilar et al., "RRT-based path planning for virtual bronchoscopy simulator," in *Proc. IEEE Int. Conf. Augmented Reality, Virtual Reality Comput. Graph.*, 2017, pp. 155–165.

[122] W. G. Aguilar, V. Abad, H. Ruiz, J. Aguilar, and F. Aguilar-Castillo, "Virtual bronchoscopy motion planner," in *Proc. IEEE Int. Conf. Electron., Elect. Eng. Comput.*, 2017, pp. 1–4.

[123] C. Fellmann and J. Burgner-Kahrs, "Implications of trajectory generation strategies for tubular continuum robots," in *Proc. IEEE/RSJ Int. Conf. Intell. Robot. Syst.*, 2015, pp. 202–208.

[124] A. Kuntz, L. G. Torres, R. H. Feins, R. J. Webster, and R. Alterovitz, "Motion planning for a three-stage multilumen transoral lung access system," in *Proc. IEEE/RSJ Int. Conf. Intell. Robot. Syst.*, 2015, pp. 3255–3261.

[125] J. Guo, Y. Sun, and S. Guo, "A training system for vascular interventional surgeons based on local path planning," in *Proc. IEEE Int. Conf. Mechatron. Automat.*, 2021, pp. 1328–1333.

[126] R. Alterovitz, S. Patil, and A. Derbakova, "Rapidly-exploring roadmaps: Weighing exploration vs. refinement in optimal motion planning," in *Proc. IEEE Int. Conf. Robot. Automat.*, 2011, pp. 3706–3712.

[127] L. G. Torres and R. Alterovitz, "Motion planning for concentric tube robots using mechanics-based models," in *Proc. IEEE/RSJ Int. Conf. Intell. Robot. Syst.*, 2011, pp. 5153–5159.

[128] L. G. Torres, R. J. Webster, and R. Alterovitz, "Task-oriented design of concentric tube robots using mechanics-based models," in *Proc. IEEE/RSJ Int. Conf. Intell. Robot. Syst.*, 2012, pp. 4449–4455.

[129] L. G. Torres, C. Baykal, and R. Alterovitz, "Interactive-rate motion planning for concentric tube robots," in *Proc. IEEE Int. Conf. Robot. Automat.*, 2014, pp. 1915–1921.

[130] J. Fauser et al., "Planning nonlinear access paths for temporal bone surgery," *Int. J. Comput. Assist. Radiol. Surg.*, vol. 13, no. 5, pp. 637–646, 2018.

[131] J. Fauser et al., "Generalized trajectory planning for nonlinear interventions," in *Comput. Assist. Robot. Endoscopy*, pp. 46–53, 2018.

[132] J. Fauser et al., "Optimizing clearance of Bézier spline trajectories for minimally-invasive surgery," in *Proc. Int. Conf. Med. Imag. Comput. And Imag. Assist. Interv.*, 2019, pp. 20–28.

[133] J. Fauser et al., "Planning for flexible surgical robots via Bézier spline translation," *IEEE Robot. Automat. Lett.*, vol. 4, no. 4, pp. 3270–3277, Oct. 2019.

[134] A. Kuntz, M. Fu, and R. Alterovitz, "Planning high-quality motions for concentric tube robots in point clouds via parallel sampling and optimization," in *Proc. IEEE/RSJ Int. Conf. Intell. Robot. Syst.*, 2019, pp. 2205–2212.

[135] L. A. Lyons, R. J. Webster, and R. Alterovitz, "Planning active cannula configurations through tubular anatomy," in *Proc. IEEE Int. Conf. Robot. Automat.*, 2010, pp. 2082–2087.

[136] D. C. Liu et al., "On the limited memory BFGs method for large scale optimization," *Math. Prog.*, vol. 45, no. 1, pp. 503–528, 1989.

[137] M. S. Bazaraa et al., *Nonlinear Programming: Theory and Algorithms*. Hoboken, NJ, USA: Wiley, 2013.

[138] F. Qi et al., "Kinematic analysis and navigation method of a cable-driven continuum robot used for minimally invasive surgery," *Int. J. Med. Robot. Comput. Assist. Surg.*, vol. 15, no. 4, 2019, Art. no. e2007.

[139] J. Guo, H. Zhao, and S. Guo, "Design a novel of path planning method for the vascular interventional surgery robot based on DWA model," in *Proc. IEEE Int. Conf. Mechatron. Automat.*, 2021, pp. 1322–1327.

[140] C. Abah, R. Chitale, and N. Simaan, "Image-guided optimization of robotic catheters for patient-specific endovascular intervention," in *Proc. IEEE Int. Symp. Med. Robot.*, 2021, pp. 1–8.

[141] M. Gao et al., "Three-dimensional path planning and guidance of leg vascular based on improved ant colony algorithm in augmented reality," *J. Med. Syst.*, vol. 39, no. 11, 2015, Art. no. 133.

[142] Z. Li et al., "Path planning for endovascular catheterization under curvature constraints via two-phase searching approach," *Int. J. Comput. Assist. Radiol. Surg.*, vol. 16, no. 4, pp. 619–627, 2021.

[143] H. Rafii-Tari et al., "Hierarchical HMM based learning of navigation primitives for cooperative robotic endovascular catheterization," in *Proc. Int. Conf. Med. Imag. Comput. And Comput. Assist. Interv.*, 2014, pp. 496–503.

[144] H. Rafii-Tari et al., "Learning-based modeling of endovascular navigation for collaborative robotic catheterization," in *Proc. Adv. Inf. Syst. Eng.*, 2013, pp. 369–377.

[145] W. Chi et al., "Learning-based endovascular navigation through the use of non-rigid registration for collaborative robotic catheterization," *Int. J. Comput. Assist. Radiol. Surg.*, vol. 13, no. 6, pp. 855–864, 2018.

[146] W. Chi et al., "Trajectory optimization of robot-assisted endovascular catheterization with reinforcement learning," in *Proc. IEEE/RSJ Int. Conf. Intell. Robot. Syst.*, 2018, pp. 3875–3881.

[147] M. Saveriano et al., "Dynamic movement primitives in robotics: A tutorial survey," 2021, *arXiv:2102.03861*.

[148] W. Chi et al., "Collaborative robot-assisted endovascular catheterization with generative adversarial imitation learning," in *Proc. IEEE Int. Conf. Robot. Automat.*, 2020, pp. 2414–2420.

[149] Y. Zhao et al., "Surgical GAN: Towards real-time path planning for passive flexible tools in endovascular surgeries," *Neurocomputing*, vol. 500, pp. 567–580, 2022.

[150] G. Trovato et al., "Development of a colon endoscope robot that adjusts its locomotion through the use of reinforcement learning," *Int. J. Comput. Assist. Radiol. Surg.*, vol. 5, no. 4, pp. 317–325, 2010.

[151] V. Mnih et al., "Human-level control through deep reinforcement learning," *Nature*, vol. 518, no. 7540, pp. 529–533, 2015.

[152] T. Behr et al., "Deep reinforcement learning for the navigation of neurovascular catheters," *Curr. Directions Biomed. Eng.*, vol. 5, no. 1, pp. 5–8, 2019.

[153] L. Karstensen et al., "Autonomous guidewire navigation in a two dimensional vascular phantom," *Curr. Directions Biomed. Eng.*, vol. 6, no. 1, 2020.

[154] F. Meng, S. Guo, W. Zhou, and Z. Chen, "Evaluation of a reinforcement learning algorithm for vascular intervention surgery," in *Proc. IEEE Int. Conf. Mechatron. Automat.*, 2021, pp. 1033–1037.

[155] L. Karstensen et al., "Learning-based autonomous vascular guidewire navigation without human demonstration in the venous system of a porcine liver," *Int. J. Comput. Assist. Radiol. Surg.*, vol. 17, no. 11, pp. 2033–2040, 2022.

[156] J. Kweon et al., "Deep reinforcement learning for guidewire navigation in coronary artery phantom," *IEEE Access*, vol. 9, pp. 166409–166422, 2021.

[157] A. Pore et al., "Colonoscopy navigation using end-to-end deep visuomotor control: A user study," in *Proc. IEEE Int. Conf. Intell. Robot. Syst.*, 2022, pp. 9582–9588.

[158] S. Athiniotis et al., "Deep q reinforcement learning for autonomous navigation of surgical snake robot in confined spaces," in *Proc. Hamlyn Symp. Med. Robot.*, 2019, pp. 23–26.

[159] J. Ibarz et al., "How to train your robot with deep reinforcement learning: Lessons we have learned," *Int. J. Robot. Res.*, vol. 40, no. 4-5, pp. 698–721, 2021.

[160] J. García et al., "A comprehensive survey on safe reinforcement learning," *J. Mach. Learn. Res.*, vol. 16, no. 1, pp. 1437–1480, 2015.

[161] A. Pore et al., "Safe reinforcement learning using formal verification for tissue retraction in autonomous robotic-assisted surgery," in *Proc. IEEE/RSJ Int. Conf. Intell. Robot. Syst.*, 2021, pp. 4025–4031.

[162] D. Corsi et al., "Constrained reinforcement learning and formal verification for safe colonoscopy navigation," 2023, *arXiv:2303.03207*.

[163] Y. LeCun et al., "Deep learning," *Nature*, vol. 521, no. 7553, pp. 436–444, 2015.

[164] D. C. Birkhoff et al., "A review on the current applications of artificial intelligence in the operating room," *Surg. Innov.*, vol. 28, no. 5, pp. 611–619, 2021.

[165] M. G. Goldenberg et al., "Using data to enhance performance and improve quality and safety in surgery," *JAMA Surg.*, vol. 152, no. 10, pp. 972–973, 2017.

[166] A. A. Rusu et al., "Sim-to-real robot learning from pixels with progressive nets," in *Proc. Conf. Robot Learn.*, 2017, pp. 262–270.

[167] J. Schulman et al., "Proximal policy optimization algorithms," 2017, *arXiv:1707.06347*.

[168] T. Haarnoja, A. Zhou, P. Abbeel, and L. Sergey, "Soft actor-critic: Off-policy maximum entropy deep reinforcement learning with a stochastic actor," in *Proc. Int. Conf. Mach. Learn.*, 2018, pp. 1861–1870.

[169] X. Lin et al., "Softgym: Benchmarking deep reinforcement learning for deformable object manipulation," in *Proc. Conf. Robot Learn.*, 2021, pp. 432–448.

[170] Z. Li et al., "Position-based dynamics simulator of vessel deformations for path planning in robotic endovascular catheterization," *Med. Eng. Phys.*, vol. 110, 2022, Art. no. 103920.

[171] P. Dupont, N. Simaan, H. Choset, and C. Rucker, "Continuum robots for medical interventions," *Proc. IEEE*, vol. 110, no. 7, pp. 847–870, Jul. 2022.

[172] A. Pore, E. Tagliabue, M. Piccinelli, D. Dall'Alba, A. Casals, and P. Fiorini, "Learning from demonstrations for autonomous soft-tissue retraction," in *Proc. IEEE Int. Symp. Med. Robot.*, 2021, pp. 1–7.

[173] S. K. S. Ghasemipour et al., "A divergence minimization perspective on imitation learning methods," in *Proc. PMLR Conf. Robot. Learn.*, 2020, pp. 1259–1277.

[174] F. Liu, A. Garriga-Casanovas, R. Secoli, and F. Rodriguez y Baena, "Fast and adaptive fractal tree-based path planning for programmable bevel tip steerable needles," *IEEE Robot. Automat. Lett.*, vol. 1, no. 2, pp. 601–608, Jul. 2016.

[175] M. Pinzi et al., "The adaptive hermite fractal tree (AHFT): A novel surgical path planning approach with curvature and heading constraints," *Int. J. Comput. Assist. Radiol. Surg.*, vol. 14, no. 4, pp. 659–670, 2019.

[176] W. Wang et al., "A learning-based multi-RRT approach for robot path planning in narrow passages," *J. Intell. Robot. Syst.*, vol. 90, no. 1–2, pp. 81–100, 2018.

[177] J. Granna et al., "Computer-assisted planning for a concentric tube robotic system in neurosurgery," *Int. J. Comput. Assist. Radiol. Surg.*, vol. 14, no. 2, pp. 335–344, 2019.

[178] M. J. Pourmanda et al., "Navigation and control of endovascular helical swimming microrobot using dynamic programing and adaptive sliding mode strategy," *Control Syst. Des. Bio-Robot. Bio-Mechatron. Adv. Appl.*, pp. 201–219, 2019.

[179] T. A. Howell, B. E. Jackson, and Z. Manchester, "ALTRO: A fast solver for constrained trajectory optimization," in *Proc. IEEE/RSJ Int. Conf. Intell. Robot. Syst.*, 2019, pp. 7674–7679.

[180] R. Cheng et al., "End-to-end safe reinforcement learning through barrier functions for safety-critical continuous control tasks," in *Proc. AAAI Conf. Artif. Intell.*, 2019, vol. 33, no. 01, pp. 3387–3395.

[181] R. F. Prudencio et al., "A survey on offline reinforcement learning: Taxonomy, review, and open problems," *IEEE Trans. Neural Netw. Learn. Syst.*, 2023.

[182] X. You et al., "Model-free control for soft manipulators based on reinforcement learning," in *Proc. IEEE/RSJ Int. Conf. Intell. Robot. Syst.*, 2017, pp. 2909–2915.

[183] T. G. Thuruthel, E. Falotico, F. Renda, and C. Laschi, "Model-based reinforcement learning for closed-loop dynamic control of soft robotic manipulators," *IEEE Trans. Robot.*, vol. 35, no. 1, pp. 124–134, Feb. 2019.

[184] J. Liu et al., "Efficient reinforcement learning control for continuum robots based on inexplicit prior knowledge," 2020, *arXiv:2002.11573*.

[185] A. Pore et al., "On simple reactive neural networks for behaviour-based reinforcement learning," *Proc. IEEE Int. Conf. Robot. Automat.*, 2020, pp. 7477–7483.

[186] Y. Bengio et al., "Curriculum learning," in *Proc. Annu. Int. Conf. Mach. Learn.*, 2009, pp. 41–48.

[187] A. A. Transeth et al., "A survey on snake robot modeling and locomotion," *Robot.*, vol. 27, no. 7, pp. 999–1015, 2009.

[188] Y. Chen, Z. Li, W. Xu, Y. Wang, and H. Ren, "Minimum sweeping area motion planning for flexible serpentine surgical manipulator with kinematic constraints," in *Proc. IEEE/RSJ Int. Conf. Intell. Robot. Syst.*, 2015, pp. 6348–6353.

[189] J. Fras, M. Macias, Y. Noh, and K. Althoefer, "Fluidical bending actuator designed for soft octopus robot tentacle," in *Proc. IEEE Int. Conf. Soft Robot.*, 2018, pp. 253–257.

[190] R. Luo, T. Wang, Z. Shi, and J. Tian, "Design and kinematic analysis of an elephant-trunk-like robot with shape memory alloy actuators," in *Proc. IEEE Adv. Inf. Technol., Electron. Automat. Control Conf.*, 2017, pp. 157–161.

[191] Y. Hu, L. Zhang, W. Li, and G.-Z. Yang, "Design and fabrication of a 3-D printed metallic flexible joint for snake-like surgical robot," *IEEE Robot. Automat. Lett.*, vol. 4, no. 2, pp. 1557–1563, Apr. 2019.

[192] S. Kolachalama et al., "Continuum robots for manipulation applications: A survey," *J. Robot.*, vol. 5, no. 41, 2020, Art. no. eaaz9239.

[193] E. W. Hawkes et al., "A soft robot that navigates its environment through growth," *Sci. Robot.*, vol. 2, no. 8, 2017, Art. no. eaan3028.

[194] C. Shi et al., "Shape sensing techniques for continuum robots in minimally invasive surgery: A survey," *IEEE Trans. Biomed. Eng.*, vol. 64, no. 8, pp. 1665–1678, Aug. 2017.

[195] S. K. Sahu et al., "Shape reconstruction processes for interventional application devices: State of the art, progress, and future directions," *Front. Robot. AI*, vol. 8, 2021, Art. no. 758411.

[196] X. T. Ha et al., "Robust catheter tracking by fusing electromagnetic tracking, fiber Bragg grating and sparse fluoroscopic images," *IEEE Sensors J.*, vol. 21, no. 20, pp. 23422–23434, Oct. 2021.

[197] X. T. Ha et al., "Contact localization of continuum and flexible robot using data-driven approach," *IEEE Robot. Automat. Lett.*, vol. 7, no. 3, pp. 6910–6917, Jul. 2022.

[198] X. T. Ha et al., "Shape sensing of flexible robots based on deep learning," *IEEE Trans. Robot.*, vol. 39, no. 2, pp. 1580–1593, Apr. 2023.

[199] B. F. Barata et al., "IVUS-based local vessel estimation for robotic intravascular navigation," *IEEE Robot. Automat. Lett.*, vol. 6, no. 4, pp. 8102–8109, Oct. 2021.

[200] N. Zulina et al., "Colon phantoms with cancer lesions for endoscopic characterization with optical coherence tomography," *Biomed. Opt. Exp.*, vol. 12, no. 2, pp. 955–968, 2021.

[201] G. Liao et al., "Distortion and instability compensation with deep learning for rotational scanning endoscopic optical coherence tomography," *Med. Image Anal.*, vol. 77, 2022, Art. no. 102355.

[202] C. Shi et al., "Real-time in vitro intravascular reconstruction and navigation for endovascular aortic stent grafting," *Int. J. Med. Robot. Comput. Assist. Surg.*, vol. 12, no. 4, pp. 648–657, 2016.

[203] F. Chadebecq et al., "Computer vision in the surgical operating room," *Visceral Med.*, vol. 36, no. 6, pp. 456–462, 2020.

[204] A. Rau et al., "Implicit domain adaptation with conditional generative adversarial networks for depth prediction in endoscopy," *Int. J. Comput. Assist. Radiol. Surg.*, vol. 14, no. 7, pp. 1167–1176, 2019.

Ameya Pore (Graduate Student Member, IEEE) received the B.S. degree in computer science from the Indian Institute of Science Education and Research, Pune, India. He is currently working toward the master's degree as an integrated degree in computer science, part of the Erasmus+ programme, with the University of Glasgow, Glasgow, U.K., and joint doctoral program in biomedical engineering and computer science with the Altair Robotics Lab, University of Verona, Verona, Italy, and the Universitat Politècnica de Catalunya, Barcelona, Spain.

He was a Visiting Student with the National University of Singapore, Singapore. He is currently an ESR with the MSCA ATLAS project.

Zhen Li (Graduate Student Member, IEEE) received the B.Eng. degree in intelligent science and technology from Nankai University, Tianjin, China, in 2017. From 2017 to 2019, she continued with the M.Sc. European master's degree in advanced robotics (EMARO+) with the Warsaw University of Technology Warsaw, Poland, and Ecole Centrale de Nantes, Nantes, France. She is currently a double Ph.D. student as ESR in bioengineering with the MSCA ATLAS project under European Union Innovative Training Network.

She is currently with NearLab, Politecnico di Milano, Milan, Italy, and with MISIT Lab, TU Delft, Delft, The Netherlands.

Diego Dall'Alba received the master's degree with honors in "Intelligent and multimedia systems", and the Ph.D. degree in computer science from the University of Verona, Verona, Italy, in 2010 and 2014, respectively.

He is currently an Assistant Professor (tenure track), working on ARS and ATLAS projects. Since 2008, he is Member of the Altair robotics laboratory. He has been involved in four European projects: AccuRobAs, Safros, ISUR, and MURAB. In 2012, he was Visiting Researcher with the University of British Columbia, Vancouver, BC, Canada.

Alicia Casals Gelpí (Senior Member, IEEE) received the Ph.D. degree in computer vision from the Polytechnic University of Catalonia (UPC), Barcelona, Spain, in 1983.

She is a Founder of the company RobSurgical Systems. She has been the Head of the Robotics and Vision group with CREB-UPC. Since 2018, she has been the President of the Science and Technology Section, Institut d'Estudis Catalans. Since 1991, she has been a Professor with UPC. In 1978, she was an Industrial Engineer with UPC.

Dr. Gelpí has been a Driving Member of the European Robotics Network and a Member of its governing team, from 2001 to 2008. From 2008 to 2009, she was a Vice President of the IEEE Robotics and Automation Society, and President of the Technical Committee on Biorobotics of the IEEE Engineering in Medicine and Biology Society, from 2017 to 2018.

Albert Hernansanz received the bachelor's and Ph.D. degrees in computer engineering from Universitat Autònoma de Barcelona, Bellaterra, Spain, in 2002.

He is currently involved in the SARAS research project developing cognitive-based control for auxiliary autonomous surgical robots. He is also the Co-Founder of SurgiTrainer, a spin-off of the UPC, IBEC, and Hospital de Sant Pau. Since 2000, he has been with the Universitat Politècnica de Catalunya and with the Institute of Bioengineering of Catalonia.

Jenny Dankelman (Member, IEEE) received the M.Sc. degree in mathematics, with a specialization in system and control engineering, from the University of Groningen, Groningen, The Netherlands, in 1984, and the Ph.D. degree in dynamics of the coronary circulation from the Delft University of Technology, Delft, The Netherlands, in 1989.

She is a Professor in Minimally Invasive Surgery and Interventional Techniques (MISIT) with the Delft University of Technology. In 2001, she was a Antoni van Leeuwenhoek Chair and shortly after she became Head of the MISIT group. She cooperates with several hospitals, such as Leiden UMC, Erasmus MC Rotterdam, and the University Medical Center Amsterdam.

Dr. Dankelman was a recipient of the Royal award of Knight in the Order of the Netherlands Lion, and in 2019, she became Member of the Royal Netherlands Academy of Arts and Sciences.

Elena De Momi (Senior Member, IEEE) received the M.Sc. degree in biomedical engineering and the Ph.D. degree in bioengineering from Politecnico di Milano, Milan, Italy, in 2002 and 2006, respectively.

She is currently an Assistant Professor with Politecnico di Milano, Milan, Italy.

Dr. Momi was an Associated Editor for IEEE ICRA, IROS and BioRob, and Area Chair of MICCAI, from 2016. She is currently a Publication Co-Chair of ICRA 2023. She is PI for POLIMI of the EDEN2020 project and of ATLAS project and co-PI of the ARTERY project. She has been Evaluator and Reviewer for the European Commission in FP6, FP7, and H2020.

Paolo Fiorini (Life Fellow, IEEE) received the Laurea degree in electronic engineering from the University of Padova, Padua, Italy, the M.S.E.E. degree from the University of California at Irvine, Irvine, CA, USA, and the Ph.D. degree in mechanical engineering from the University of California at Los Angeles, Los Angeles, CA, USA.

He is currently a Full Professor with the University of Verona, Verona, Italy. From 1977 to 1985, he was with companies in Italy and in the USA, developing microprocessor-based controllers. From 1985 to 2000, he was with NASA Jet Propulsion Laboratory, California Institute of Technology, Pasadena, CA, USA, where he worked on autonomous and teleoperated systems. In 2001, he returned to the University of Verona. In 2001, he founded the ALTAIR robotics laboratory and is involved in the European Framework programs FP6, FP7, H2020, and ERC.

Dr. Fiorini' was a recipient of the IEEE Fellow (2009) and NASA Technical Awards.

Arianna Menciassi (Fellow, IEEE) received the bachelor's degree in physics from the University of Pisa, Pisa, Italy, in 1995, and the Ph.D. degree from the Scuola Superiore Sant'Anna (SSSA), Pisa, Italy, in 1999.

She is a Professor of bioengineering and biomedical robotics with the SSSA. Since 2014, she has been a Visiting Professor with different universities in France, such as Pierre and Marie Curie and Besancon University. Since 2018, she has been the Co-Ordinator of the Ph.D. with the BioRobotics Institute and she is a Team Leader of the "Surgical Robotics & Allied Technologies" Area. In 2019, she was a Vice-Rector of the SSSA.

Emmanuel Vander Poorten (Member, IEEE) received the M.S. degree in mechanical engineering from KU Leuven, Leuven, Belgium, in 2000, and the Ph.D. degree in mechatronics from Kyoto University, Kyoto, Japan, in 2007.

He is an Associate Professor with the Faculty of Engineering Technology of KU Leuven, where, since 2010, he has been coordinating the activities of the Robot-Assisted Surgery group. He has been heavily involved in several projects: RADHAR, SCATh, CASCADE, ARTERY, EurEyeCase, and ATLAS.